A MATHEMATICAL MODEL OF A GAS KICK WHEN DRILLING IN DEEP WATERS

by

Otto Luis Alcantara Santos

T-2703

A thesis submitted to the Faculty and the Board of Trustees of the Colorado School of Mines in partial fulfillment of the requirements for the degree of Master of Science (Petroleum Engineering).

Golden, Colorado

Date DECEMBER 1, 1982

Signed: Otto L. A. Santos

Approved: Bill Mitchell 12/3/82
B. J. Mitchell
Thesis Advisor

Golden, Colorado

Date December 3, 1982

Craig W. Van Kirk
C. W. Van Kirk
Head, Department of
Petroleum Engineering

ABSTRACT

The central part of this work is the derivation of a mathematical model which simulates the surface pressures generated during the removal of a kick while drilling in deepwater.

This model assumes that the kick is gas which is dispersed within the drilling fluid as small bubbles.

Eleven critical kick removal variables are studied.

TABLE OF CONTENTS

TABLE OF CONTENTS (Cont'd)

LIST OF FIGURES

LIST OF FIGURES (Cont'd)

LIST OF TABLES

ACKNOWLEDGEMENTS

The author is gratefully indebted to Petroleo Brasileiro S.A. (Petrobras), which made his stay here possible.

The author wishes to express his gratitude to Dr. B. J. Mitchell whose time and supervision made this work possible.

Sincere appreciation is extended to Prof. C. S. Aldrich for his suggestions and assistance during the elaboration of this work.

Appreciation is also extended to Prof. J. D. Wright and Prof. D. I. Dickinson for serving on the thesis committee.

Finally, the author wishes to express his thankfulness to his wife Janete and to his daughter Patricia whose love and conviviality made this investigation possible. To them, the author dedicates this work.

INTRODUCTION

When the hydrostatic pressure of the drilling fluid, commonly called mud, becomes less than the pressure of a formation containing a fluid, such as gas, oil or water and the permeability of the formation is moderately high, a large amount of formation fluid will flow into the wellbore. The collected fluid is commonly called a kick.

When the formation fluid is water or oil with low Gas Oil Ratio the removal of the kick is not complicated, because either fluid is only slightly compressible.

The same cannot be said for a gas kick, because the gas must be allowed to expand as the gas ascends the annulus of the wellbore.

But, if the control of the well is lost, the kick becomes a "blowout."

"Blowouts" may result in the loss of equipment or in the loss of a well. In offshore drilling, crew safety and oil spills are more critical than on land.

Blowouts without heavy loss in equipment may reflect negatively in drilling costs because of the time lost in regaining control of the well.

Good well control procedure may be achieved if the pressure behavior of the fluids in the wellbore is known as a kick ascends the wellbore.

Some depths in the wellbore are more critical than other depths. Common critical depths are the bottom of the hole, the shoe of the last casing string and the surface. The pressure variations at these depths, as a function of the displacement, produce curves which are critical in regard to the understanding of the displacement process of a kick.

Mathematical wellbore pressure simulators, consequently, serve as a tool for well control during kick removal.

The purpose of this work, then, is to present a mathematical simulator for kick removal while drilling in deep water.

Well control procedures in deep waters are different than those on land or in shallow water. A section of this work describes the most important peculiarities of deep-water well control.

The complexity of the model necessitated the writing of a computer program. The results were plotted in graphs.

These graphs were analyzed and conclusions were drawn based on the effect of each important variable, especially those intrinsically related to the proposed mathematical model.

FUNDAMENTALS OF KICK

A) CIRCULATION OF DRILLING FLUID THROUGH AN ONSHORE WELL

Figure 1 shows how the drilling fluid path through the circulation system of an onshore rig.

The mud is pumped down the inside of the drill string until it reaches the bit. The drilling fluid lubricates, cleans and cools the bit. Thereafter, it flows up inside an annulus formed by the wellbore walls and the drilling string, carrying small fragments of drilled rock to the surface where they are separated from the drilling fluid. At the surface, the mud is treated in order to remove the drilled solids incorporated in it. After treatment, the fluid is pumped back into the well.

The annulus is composed of two parts. The lower one represents the uncased section of the well. The upper one is formed of a steel casing which isolates and protects the upper drilled formations. At the upper end of the casing string (in onshore and in shallow waters this location corresponds with the surface) is the blowout preventer, or more commonly, called the BOP. The BOP plays a major role during the removal of a kick.

The BOP is a big valve which may be closed after detection of formation fluids inside the wellbore. When the

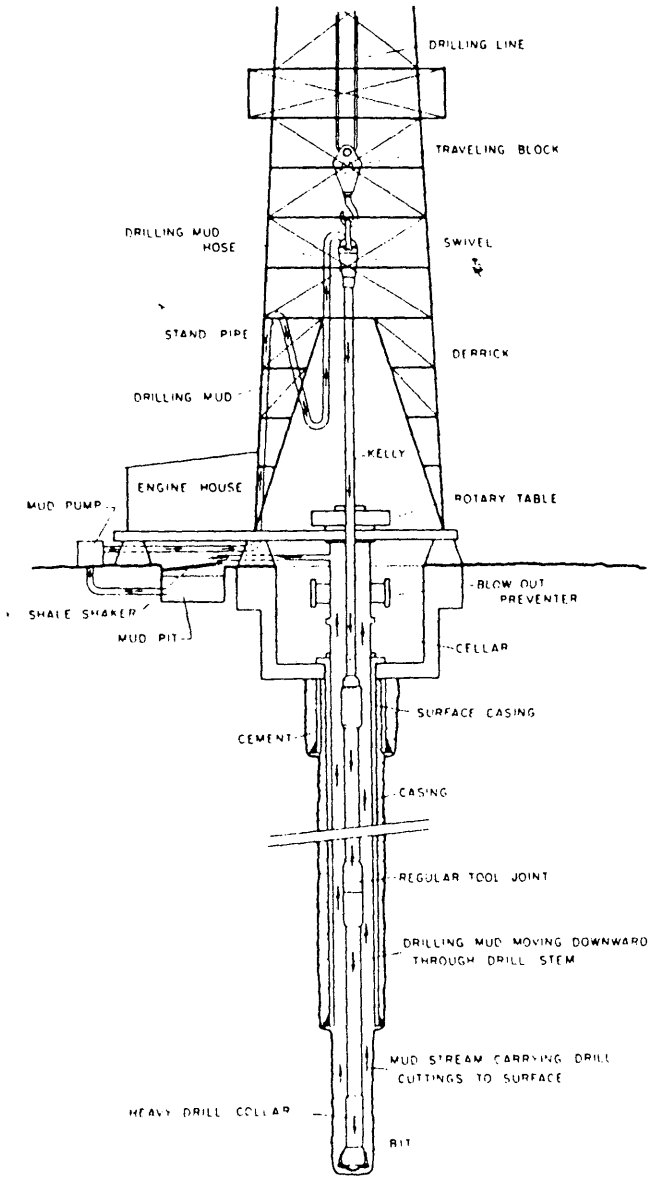

FIGURE 1 - CIRCULATION OF DRILLING FLUID THROUGH AN ONSHORE WELL (AFTER CHILINGARIAN AND VORABUTR - REF. 1)

BOP is closed, the influx of formation fluid is terminated because of a pressure increase inside the wellbore. The next step is to remove the kick from the system.

During kick removal the mud circulation path is modified. Once the BOP closes the annulus, the flow is diverted from the annulus into a parallel conduit called the choke line. At the upper end of the choke line is an adjustable choke which controls the pressure within the wellbore.

After the gas has been circulated from the wellbore and heavier mud has filled the annulus of the wellbore, the BOP is opened and the normal drilling is resumed.

B) CAUSES OF KICKS

A kick may occur if the hydrostatic pressure generated by the drilling fluid is less than the pressure of the fluid within the formation interstices. The permeability of the rock and the negative differential pressure (pressure of the formation fluid less the mud pressure) are the most important variables which govern the severity of formation fluid influx.

According to Neal Adams (2) the most common causes of kicks are:

a) Insufficient mud weight - in this case the formation pressure is greater than the hydrostatic head of the

current mud as the kick was taken. This kind of kick normally occurs while drilling abnormally pressured formations.

b) Improper hole fill-up during trip - when the bit needs to be changed, the entire drill string is removed from the wellbore, causing a mud level fall and consequently a hydrostatic pressure diminution. Thereby the well must be filled regularly to avoid hydrostatic pressure reduction.

c) Swabbing - when the drill string is pulled out of the wellbore, negative pressures are induced, reducing the pressure opposite the formations. The severity of this pressure reduction involves the hole geometry, pipe pulling speed and mud properties.

d) Cut mud - a reduction of the mud density occurs when gas contaminates the mud.

e) Lost circulation - if the hydrostatic pressure gradient overcomes the fracture gradient of the unprotected formation, it will fracture and the drilling fluid will be lost through the paths generated within the formation. Consequently the mud level will fall within the wellbore, causing a hydrostatic pressure reduction.

C) WELL KILLING METHODS

The literature reports several procedures to remove a kick from the wellbore. The majority of these methods adopts the concept of constant bottom hole pressure. These methods require the pressure at the bottom of the well be constant during kick removal. As a precaution to prevent further influxes of formation fluids into the wellbore and an enlargement of the kick, this pressure is maintained at a slightly higher level than the formation pressure.

The more popular kick removal methods are the following:

- Driller's method. This method comprises two circulations. During the first one the gas is displaced from the wellbore at constant bottom hole pressure by the current mud. In the second circulation the current mud is replaced by a heavier one which is able to produce a hydrostatic pressure greater than the formation pressure. This method is the simplest to understand and to teach to rig crews but may cause highest pressures inside the wellbore during kick removal.
- Wait and weight method. It uses just one circulation. The kick fluid is displaced by the weighted mud. This method normally leads to the lowest pressures inside the

system but requires more complicated mathematical calculations. If too much time is consumed increasing the mud weight before the removal of the kick, the pressure inside the system may become excessive.

Regardless of the method used to displace a gas kick, two important aspects must be observed as pointed out in reference (3):

The pressure opposite the kick generating formation must be slightly higher than its pore pressure in order to avoid further influxes.

The fracture resistance strengths of all formations in the uncased part of the well and the burst resistance of the casing must be greater than the pressures developed inside the system during the removal of the kick.

DEEPWATER KICK CONTROL

A) CIRCULATION OF DRILLING FLUID THROUGH A DEEPWATER WELL

Kick removal in deepwater differs in some aspects from kick removal on shore or in shallow water.

The rig equipment is installed on a floater (drillship or semisubmersible). The upper end of the casing string is not located at the surface but at the seabed. The blowout preventer is now at the seabed just above the casing head. In deepwater drilling the mud flows up from the seabed to the drillship through an annulus formed by the drill string and the drilling riser. This is illustrated in figure 2.

When a kick is detected, the wellbore is shut-in with the blowout preventer. Thereafter, the mud can no longer flow up the annular space but must rise inside the choke line (figure 3). The removal of the kick is performed through the choke line.

B) SOME IMPORTANT ASPECTS DURING KICK REMOVAL FROM A FLOATER

Fracture gradients observed in deep water are less than those existing in shallow waters or on land at equivalent depths. This difference results from the fact that the overburden stress in deep water is less than that

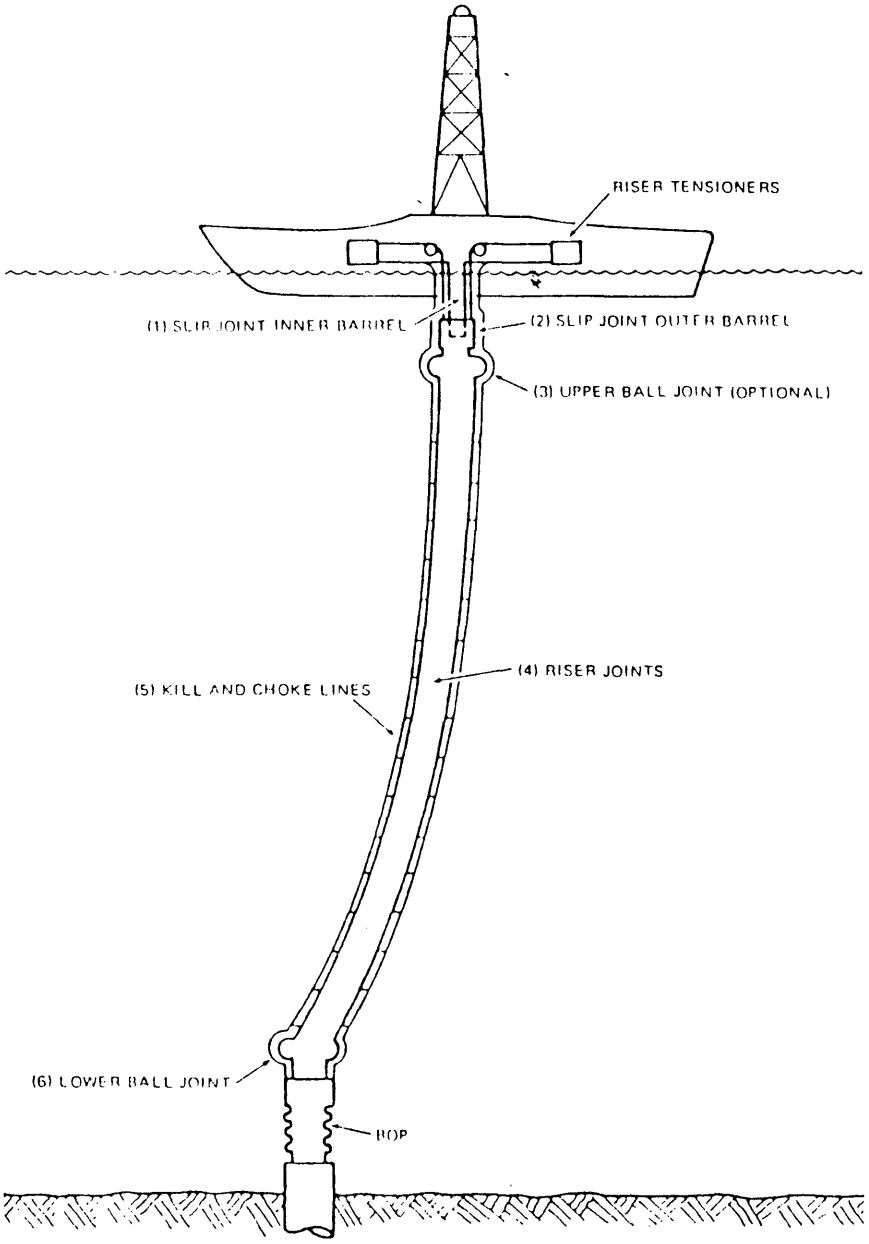

FIGURE 2 - RISER SYSTEM FOR A FLOATING DRILLING RIG (AFTER SHEFFIELD REF. 2)

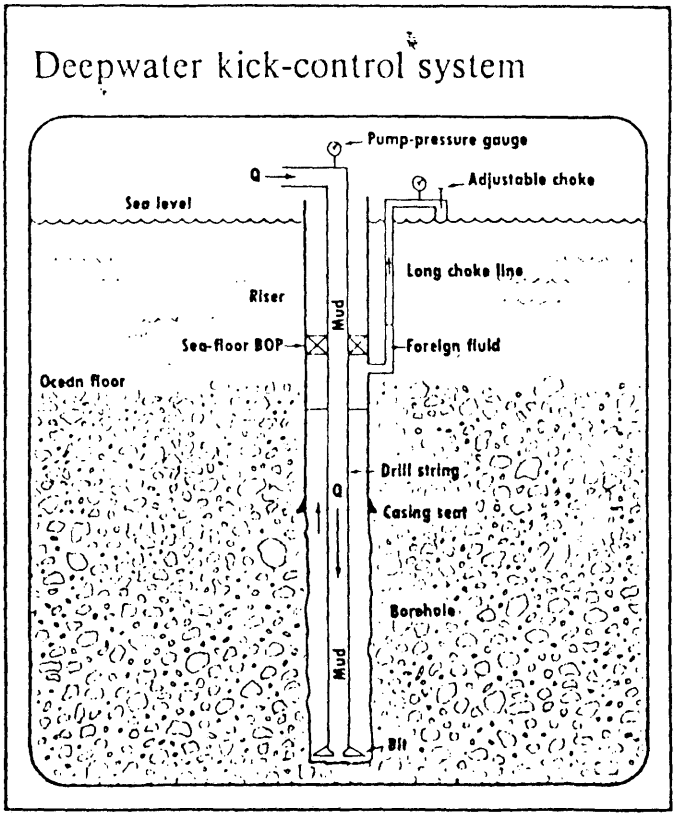

FIGURE 3 - DEEPWATER KICK CONTROL
(AFTER ANGEL - REF. 5)

existing in shallow waters or on land. Figure 4 illustrates the behavior of fracture gradient in several water depths. This reduction of fracture gradient in deepwaters creates difficulties in handling kicks from a floater.

The pressure required to circulate through the choke line is another important aspect that must be taken into account during kick removal. This pressure, if combined with other pressures may produce a total pressure within the wellbore which may be sufficient to fracture the weaker formations. The choke line pressure can be measured directly on the rig site as proposed by Goins (6) or estimated through mathematical models, such as, the Power-law Model or Bingham Model (7). Figure 5 shows the choke line pressure loss against flow rate for 2", 2.5" and 3" choke line inside diameters.

Finally, another important aspect to be observed during gas kick removal is the rapid change in hydrostatic pressure as the gas enters the choke line and later as the gas leaves the choke line. This must be observed by the operator in order to avoid secondary kicks or formation fracturing (8).

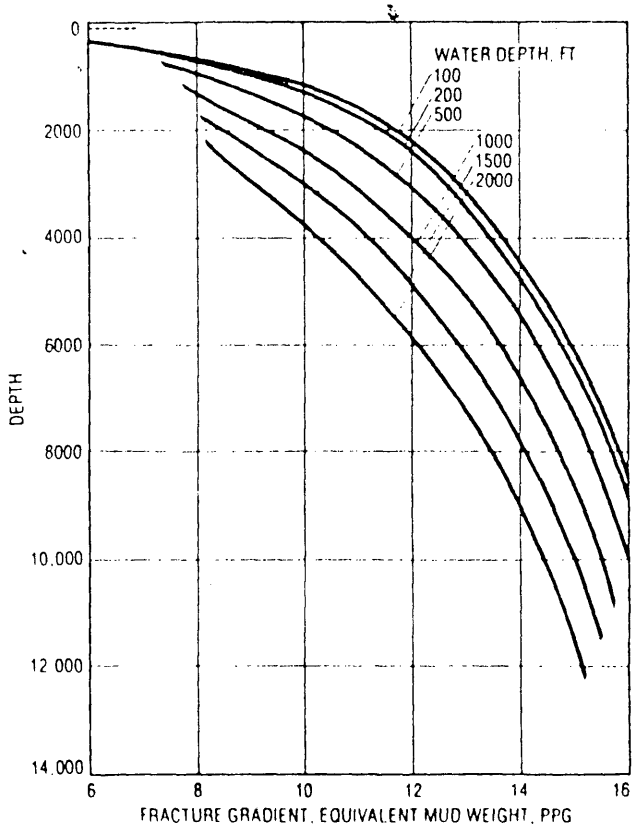

FIGURE 4 - WATER DEPTH AND FRACTURE GRADIENT (AFTER ADAMS - REF. 2)

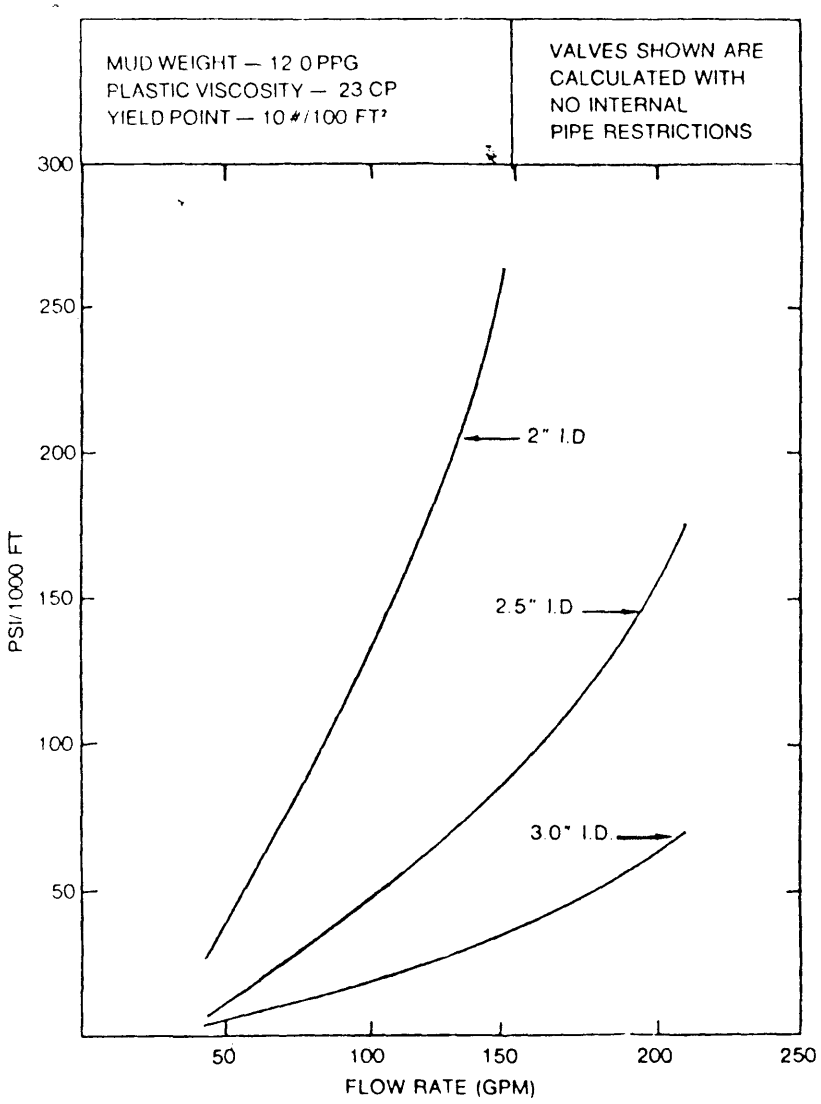

FIGURE 5 - EFFECT OF CHOKE LINE SIZE AND FLOW RATE ON FRICTION PRESSURE GRADIENT (AFTER ADAMS - REF. 2)

MATHEMATICAL MODEL

A) PREVIOUS WORKS

The first attempt to model a kick displacement was developed by Records (9). He utilized the constant bottom hole pressure concept and gas expansion within the annulus to calculate the annular pressures. After Records, several other investigators studied the pressure behavior within the wellbore during kick removal.

In 1968, Lewis and Leblanc (10) presented an analysis of annular pressure variation during a gas kick displacement. This model became very popular; however, certain assumptions were imposed in deducing the mathematical model, limiting its use. The most important limitations were:

- The model assumed no liquid hold-up or gas slip velocity.
- It was based on a frictionless system.
- The gas kick was assumed to be a discrete bubble with clean leading and trailing edges.
- The model considered constant annular geometry.

They also presented a comparison between their model's pressure profile and the annular pressure profile for an actual well (figure 6). The disagreement was attributed to the circulating friction loss in the annulus

and to the gas slip velocity.

Records (11) improved the preceding model by introducing the frictional pressure loss within the annulus. Figure 7 shows the effect of frictional pressure loss on the annular pressure profile.

Rader, Bourgoyne and Ward (12) presented an annular bubble rise velocity correlation based on a large gas bubble rising through the mud with liquid backflow occupying an area opposite the bubble.

In 1976, Stanbery (13) presented a very accurate mathematical model for an onshore well. He took into account the laminar and turbulent flow characteristics of a Bingham plastic mud, the gas slip velocity, the liquid hold-up and the frictional pressure loss within the two-phase flow region. He assumed that the gas was dispersed as individual bubbles in the drilling fluid. The temperature was assumed constant and the driller's method was adopted. Stanbery established his model assuming certain conditions existing on an actual kick displacement in a full scale well located at Louisiana State University, Baton Rouge, Louisiana. The simulation results showed a very good agreement with the actual data.

In 1977, Ilfrey, Alexander, Neath, Tannich and Eckel (8) simulated a deepwater floating kick removal. They

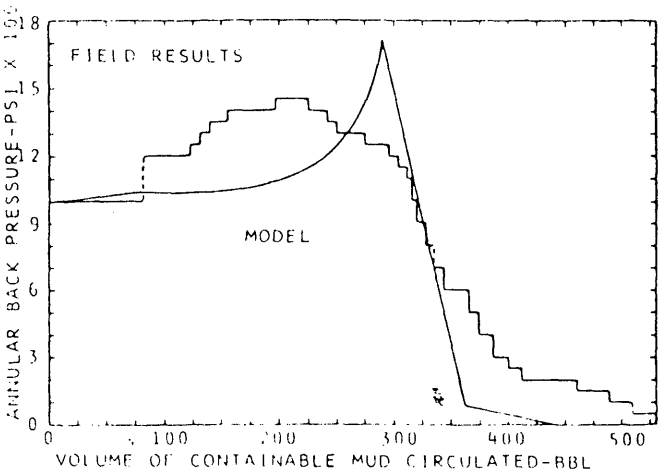

FIGURE 6 - LEWIS' AND LEBLANC'S MODEL (AFTER LEWIS AND LEBLANC - REF. 10)

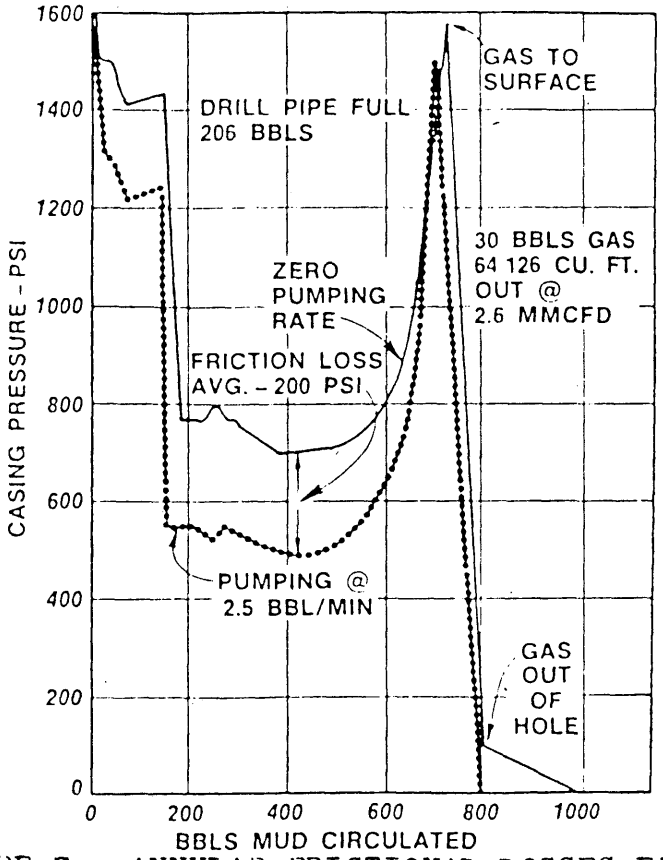

FIGURE 7 - ANNULAR FRICTIONAL LOSSES EFFECT (AFTER RECORDS - REF. 11)

pointed out the frictional pressure loss and the rapid rise in the surface pressure after the gas enters the choke line. However, their model considered the kick as being a discrete gas bubble with clean leading and trailing boundaries.

B) MODEL ASSUMPTIONS AND CONSIDERATIONS

This new model which has been developed by the author considers the gas kick distributed through the mud (continuous phase) as discrete bubbles forming a region of two-phase mixture. Gas slip velocity and gas fraction (volume of the mixture occupied by gas) are also considered.

Frictional pressure losses are considered within the single-phase regions, where only mud flows, as well as within the two-phase region.

It assumes the gas is of constant composition and no phase change occurs during kick removal.

The mud exchanges heat with the surrounding formation and a geothermal gradient is included. The sea temperature is assumed to be $50^{\circ}F$. The gas bubbles are in thermic and pressure equilibrium with the surrounding mud.

For calculation convenience, the annular geometry is assumed constant over the total well depth. Also, it is assumed that the choke line is filled with current mud when the shut-in pressures are taken.

The driller's method is used during kick removal because changes in the mud weight could mask the effect of the variables to be studied.

The constant bottom hole pressure concept is applied. During kick removal, a pressure equal to the kick generating formation pressure plus a safety margin of 150 psi is kept constant at the bottom of the well.

C) BUBBLE FLOW PATTERN

According to Wallis (14) the bubble flow pattern is characterized by a suspension of discrete gas bubbles in a continuous liquid phase. This flow regime is comprised of very small diameter bubbles to large ones filling almost the total cross sectional area of the annulus. If the bubbles are so large that they assume a cylindrical shape filling almost the entire cross area of the annulus, they are classified into another flow pattern called slug flow. Figure 8 illustrates the bubble and slug flow pattern.

Gas kicks normally occur while drilling permeable formations of various pore diameters. For this reason the diameters of the bubbles formed are very diverse. As will be seen in section E, bubble rise velocity through the surrounding liquid is a function of bubble diameter. Larger bubbles rise faster than smaller ones. This implies a bubble size distribution through the two-phase

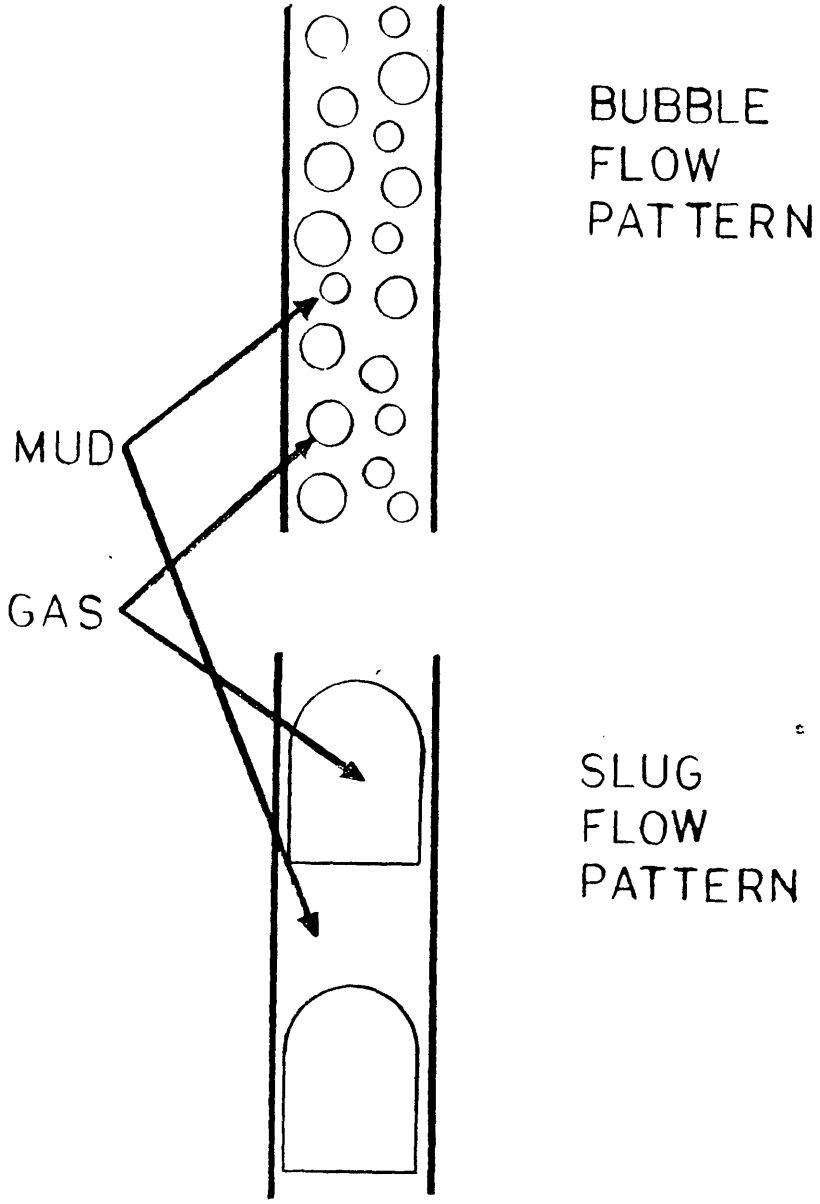

FIGURE 8 - BUBBLE AND SLUG PATTERNS

region as shown in figure 9. The largest bubbles are at the top of the two-phase flow region.

The tendency of bubbles to coalesce is reduced by this bubble distribution and the mud characteristics. This implies that the bubble flow pattern is stable or fully developed during kick removal and is a valid consideration. Stanbery (13), using this approach, obtained good agreement with field data.

D) PRELIMINARY CALCULATIONS

When the kick is detected within the wellbore, the BOP is closed and the pressures within the drill string and the annulus are recorded. The formation pressure can be found using the equation:

$$PF = SIDPP + GMH \times FD \qquad (1)$$

Where

PF - formation pressure

SIDPP - shut-in drillpipe pressure

GMH - mud hydrostatic gradient

FD - depth of the kick formation

This work, as does the above equation, assumes the depth of the kick generating formation coincides with the total depth of the well.

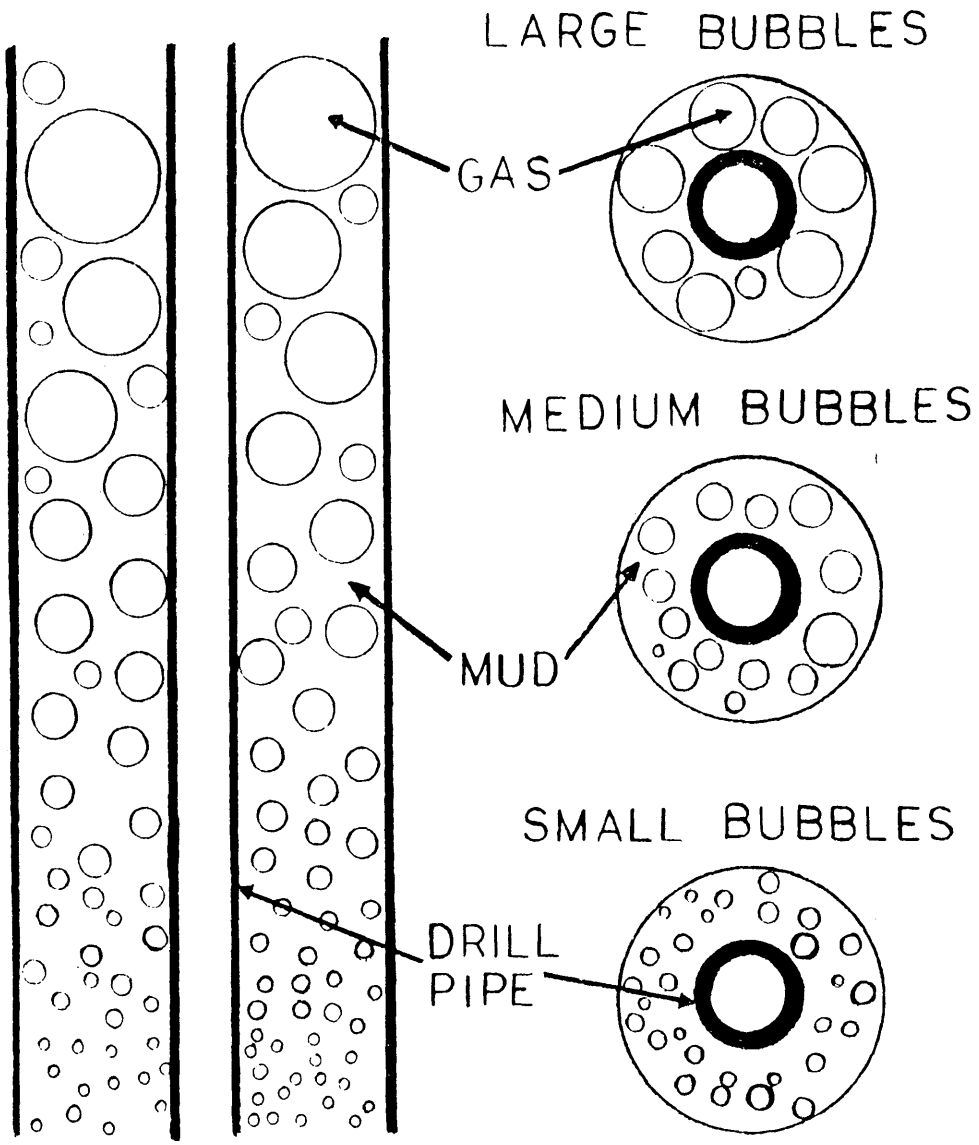

FIGURE 9 - BUBBLE DISTRIBUTION WITHIN AN ANNULUS

The average gas fraction ($\overline{XG}$) is the ratio between the gas volume and the volume of the two-phase region. Its initial value ($\overline{XG}_1$) is difficult to obtain in an actual situation. If the gas injection period is recorded by devices installed on the floater, the gas flow rate (GFR) can be estimated by the ratio between the kick size (KS) and injection period. The kick size (KS) is the amount of gas which entered the wellbore before its closure.

Initial average gas fraction may be estimated by

$$\overline{XG}_1 = \frac{GFR}{GFR + NCR} \tag{2}$$

Where NCR is the normal circulating flow rate.

The formation pressure and the initial average gas fraction are useful to calculate:

1) Initial length of the kick (LK_1) or initial length of the two-phase region.

$$LK_1 = \frac{KS}{AC \times \overline{XG}_1} \tag{3}$$

Where AC is the annular capacity

2) Mean pressure inside the two-phase region. This pressure plays a central role in this model, because the gas properties are computed at the mean pressure. For static conditions the mean

pressure can be computed by:

$$\overline{P}_1 = \frac{1}{\overline{XG}_1 \times A_1 \times LK_1} \times \left(PB_1 - \frac{\overline{XL}_1 \times \rho_L}{\overline{XG}_1 \times A_1} \right) \times$$

$$\left(e^{-(\overline{XG}_1 \times A_1 \times LK_1)-1} \right) - \left(\frac{\overline{XL}_1 \times \rho_L}{\overline{XG}_1 \times A_1} \right) \quad (4)$$

Where: $\overline{P}_1$ - mean pressure at initial conditions (static conditions)

PB_1 - pressure at the lower boundary of two-phase region

ρ_L - mud density

$\overline{XL}_1$ - initial average liquid fraction. It is equal to $1-\overline{XG}_1$

A_1 - $(K \times \gamma_g) / (T_1 \times Z_1)$

K - constant independent of the gas

γ_g - gas specific weight

T_1 - initial temperature at the center of the two-phase region

Z_1 - gas compressibility factor at initial conditions.

This equation is derived in appendix A.

3) Initial average gas density ($\overline{\rho}_g$). The equation of state for a real gas is given by:

$$P \times V = Z \times n \times R \times T \qquad (5)$$

Where: P - pressure

V - volume

Z - compressibility factor of the gas

n - number of moles

R - gas constant

T - temperature

The gas density is defined as mass of gas divided by the volume of gas

$$\bar{\rho}_g = M_g/V \qquad (6)$$

The number of moles is computed by dividing the mass of the gas by its molecular weight. The molecular weight of gas is defined as its specific gravity times the molecular weight of air. So,

$$n = M_g \; / \; 28.96 \times \gamma_g \qquad (7)$$

Substituting (6) and (7) into (5) the following equation is found

$$\bar{\rho}_g = \frac{\bar{P} \times 28.96 \times \gamma_g}{Z \times R \times T} \qquad (8)$$

Recognizing 28.96/R as K and $(\gamma_g \times K)/(T \times Z)$ as A, the initial gas density can be determined by:

$$\overline{\rho}_{gl} = \overline{P} \times A_1 \qquad (9)$$

4) Kick weight (W). This value is important because it will influence the later phase of the gas displacement while the gas is leaving the system

$$W = \overline{\rho}_g \times KS \qquad (10)$$

5) Pressure at the upper boundary of the two-phase region (PT_1). The pressure drop across the two-phase flow region can be calculated by the following formula derived in appendix A

$$DP_1 = \overline{P}_1 \times \overline{XG}_1 \times A_1 \times LK_1 + (\overline{XL}_1 \times \rho_L) \times LK_1 \qquad (11)$$

The pressure at the top of the two-phase flow is given by

$$PT_1 = PB_1 - DP_1 \qquad (12)$$

All these values are useful to determine the surface pressure at shut-in conditions. It is computed by

$$PS_1 = PT_1 - GMH \times (FD - LK_1) \qquad (13)$$

The PS_1 value calculated by equation 13 must be almost the same as that indicated by the gauge installed on the choke manifold provided the initial average gas

fraction has been estimated correctly. If it is desirable to obtain the pressure acting on the wellhead at shut-in conditions, the following equation may be used

$$PW_1 = PC_1 + GMH \times WD \qquad (14)$$

Where WD is the water depth.

The initial conditions can be seen in figure 10.

E) GAS SLIP CORRELATIONS

Much experimental work has been performed to assist the development of a mathematical formulation for the gas rise velocity through a flowing liquid. There are some publications detailing the flow through tubes (15, 16) and through annuli (12, 17, 18).

Rader, Bourgoyne, and Ward (12) have found that a bubble in slug flow rises at a velocity given by

$$VS = 10 \times C_1 \sqrt{XG} \times C_2 \times C_3 \times \sqrt{\frac{(RO+RI) \times (\rho_L - \bar{\rho}_g)}{\rho_L}} \qquad (15)$$

Where: VS - bubble slip velocity (ft/sec)

C_1 - constant accounting for viscous characteristics of the mud

C_2 - constant accounting for the mud flow velocity

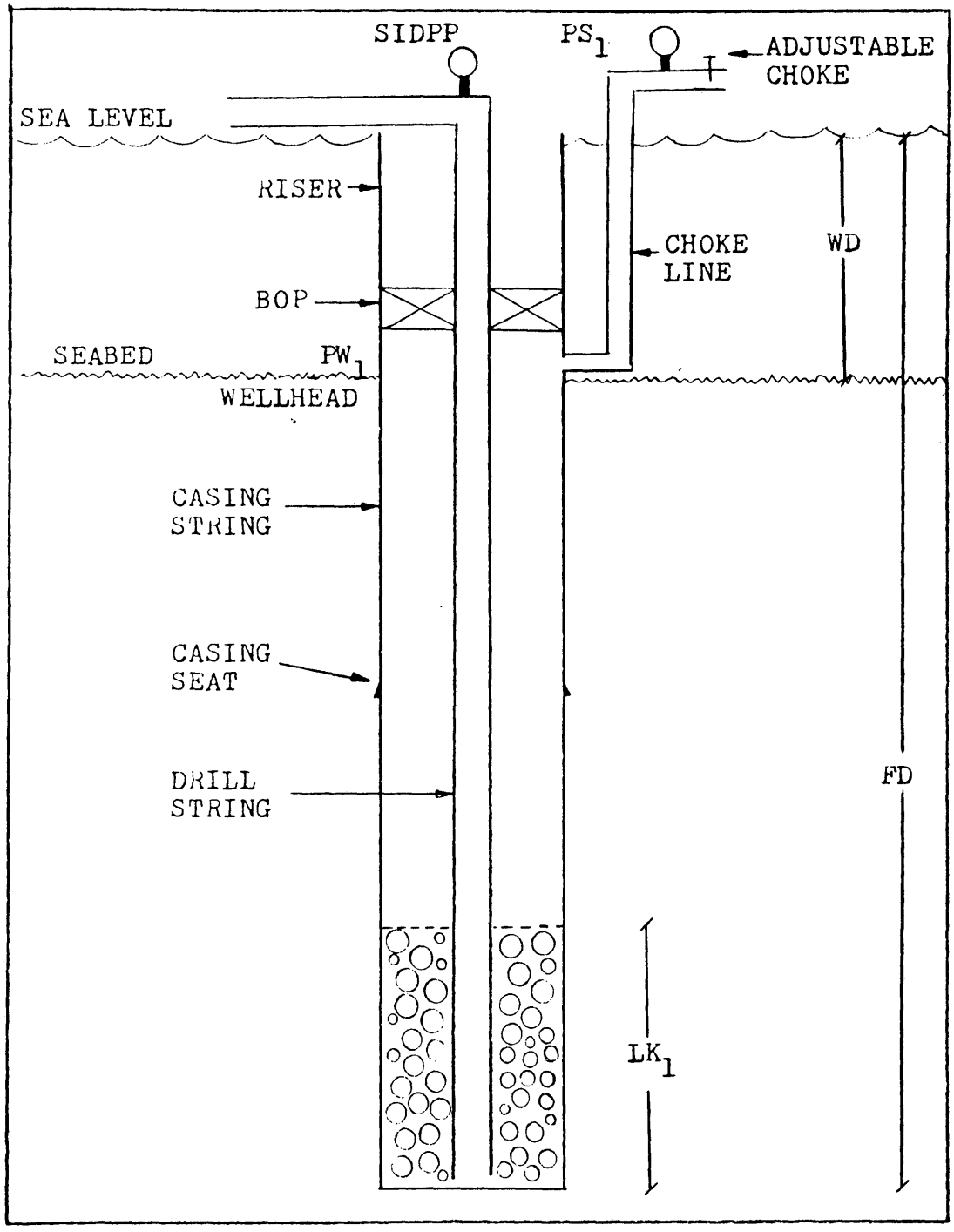

FIGURE 10 - INITIAL CONDITIONS

C_3 - constant accounting for bubble expansion

RO - outside drillpipe radius (inches)

RI - inside casing radius or wellbore radius (inches)

The total bubble velocity is given by

$$VB = VS + VM \tag{16}$$

Where VM is the mud velocity inside the annulus.

Another gas-rise correlation for slug flow within an annulus has been developed by Griffith (18). His experimental results, obtained in reduced models, showed that gas-rise velocity may be expressed by

$$VB = K1 \times \sqrt{\frac{g \times DO \times (\rho_L - \bar{\rho}_g)}{\rho_L}} + (1 + K2) \times VM \tag{17}$$

Where: g - acceleration due to gravity

DO - inside diameter of the casing or wellbore diameter

K1 - constants

K2 - constants

The constant K1 and K2 are functions of the duct geometry and are presented in figure 11. In order to use this correlation in a computer program these curves were fitted

to a third degree polynomial.

$$K1 = .345 - .037 \times R + .235 \times R^2 - .134 \times R^3 \quad (18)$$

$$K2 = .200 - .041 \times R + .010 \times R^2 - .033 \times R^3 \quad (19)$$

R represents the ratio between the small diameter DI and the big diameter DO of the annulus.

Both gas slip velocity correlations were developed for slug flow. Stanbery (13) proposed that equation 17 could be used also for bubble flow provided that DO was replaced by the bubble diameter.

Rader (17), using a full scale well at Louisiana State University, reported average velocities of the bubbles rising from the bottom of the well to the surface. The test parameters were:

Tubing outside diameter (DI)	:	2.875 inches
Casing inside diameter (DO)	:	4.887 inches
Mud density	:	8.6 pounds per gallon
Gas density	:	negligible
Mud velocity	:	0 feet/sec
Mud plastic viscosity	:	12.6 centipoise

Table 1 presents the calculated gas-rise velocity for each Griffith's and Rader's correlation and the value recorded by Rader.

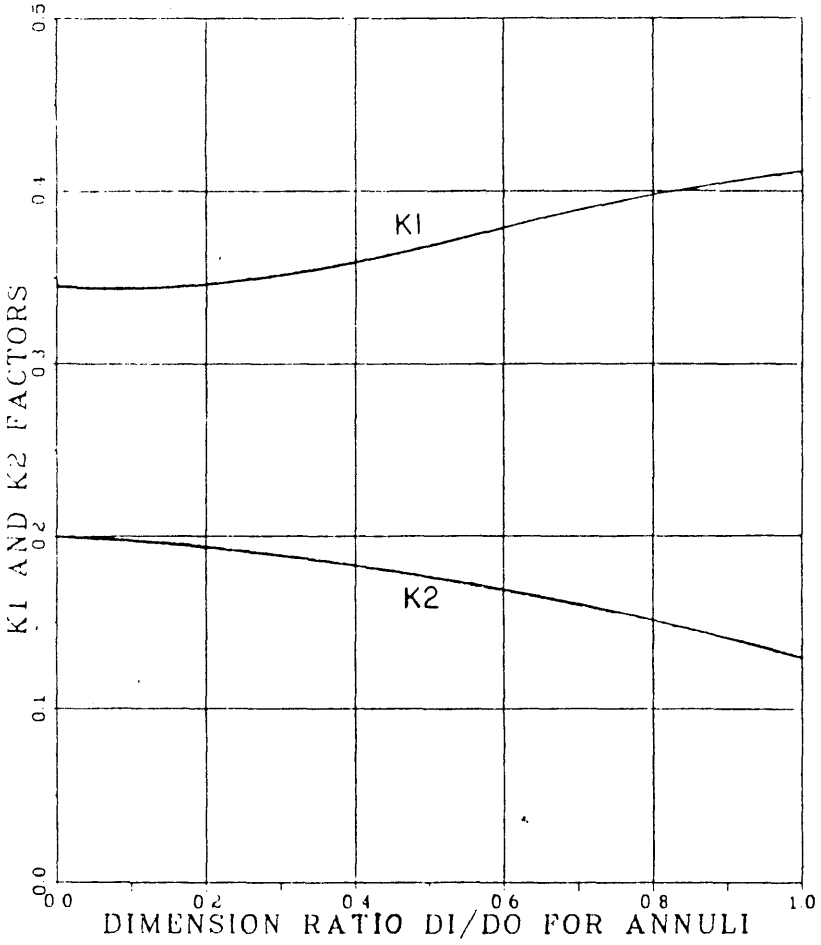

FIGURE 11 - K1 AND K2 CONSTANTS

Correlation	Flow pattern	Gas-rise velocity (ft/sec)
Rader et al.	Slug	1.27
Griffith	Slug	1.37
	Bubble	.55
Value measured by Rader		.50

Table 1 - Gas-rise Velocity Correlation

The bubble diameter used in the calculations was the difference between RO and RI.

Based on these results, Griffith's correlation was used for the gas rising velocity.

F) KICK DISPLACEMENT THROUGH THE ANNULUS

This phase begins when the rig pump is turned on and ends when the upper boundary of the two-phase flow reaches the subsea wellhead.

The positions of the boundaries of the two-phase flow region are determined using the same approach described in reference 13.

As already shown, the largest bubbles are at the top of the two-phase region. Therefore, the velocity of the

upper boundary can be calculated using equation 17 if DO is the difference between the internal casing radius or wellbore radius and the drillpipe radius. This difference corresponds to the maximum bubble diameter possible if the bubble flow is fully developed.

The position of the upper boundary may be computed by

$$HUB_t = HUB_{t-1} + VUB_{t-1} \times TI \qquad (20)$$

Where: HUB - height of the upper boundary

VUB - velocity of the upper boundary

TI - time increment

The subscripts t and t-1 refer to current and preceding time steps respectively.

At the lower end of the two-phase flow region, very small bubbles are expected. In other words, DO approaches zero. In doing so, the first term of equation 17 may be neglected if compared with the second one. Consequently, the lower boundary velocity may be expressed as

$$VLB = (1 + K2) \times VM \qquad (21)$$

The position of the lower boundary may be computed by

$$HLB_t = HLB_{t-1} + VLB \times TI \qquad (22)$$

Hence, the length of the two-phase region (LK) may be determined by

$$LK = HUB - HLB \tag{23}$$

The pressure at the lower end of the two-phase region is given by

$$PB = BHP - (GMH + GMF) \times HLB \tag{24}$$

Where GMF is the frictional pressure gradient of the mud. This gradient is calculated with the Bingham Model (7, 19). BHP is the bottom hole pressure.

The mean pressure is calculated considering the frictional pressure loss across the two-phase flow region.

$$\overline{P} = \frac{1}{\overline{XG} \times A \times LK} \times \left(PB + \frac{\overline{XL} \times \rho_L + GTPFA}{\overline{XG} \times A} \right) \times \left(e^{-\overline{XG} \times A \times LK} - 1 \right) - \left(\frac{\overline{XL} \times \rho_L + GTPFA}{\overline{XG} \times A} \right) \tag{25}$$

Where GTPFA is the frictional pressure loss gradient across the two-phase region during the displacement of the mixture through the annulus. This equation is derived in appendix A.

The average gas density ($\overline{\rho}_g$), the gas volume (GV) and the average gas fraction ($\overline{XG}$) may be calculated respectively by:

$$WK = A \times \overline{P} \tag{26}$$

$$GV = W / \rho_g \tag{27}$$

$$\overline{XG} = GV / TPV \tag{28}$$

Where TPV is the two-phase volume.

It must be noted that prior to computing the mean pressure it is necessary to have the value of XG, A and GTPFA. As a consequence, an iterative process is necessary to calculate the mean pressure.

The frictional pressure loss gradient in the two-phase region can be computed treating the mixture as a homogeneous fluid (14, 20, 21).

According to Orkiszewski (22), for bubble flow pattern, the mixture frictional pressure loss gradient can be computed by:

$$GTPFA = \frac{f \times VL^2 \times \rho_L}{2 \times g_c \times DE} \tag{29}$$

Where: f - Moody friction factor

VL - average liquid velocity within the mixture

g_c - conversion factor

DE - equivalent diameter (DO-DI)

The friction factor is a function of the Reynolds Number defined as

$$RN = \frac{DE \times VL \times \rho_L}{\mu_L} \tag{30}$$

Where μ_L is the liquid phase viscosity.

The average liquid velocity within the mixture is given by equation 31.

$$VL = \frac{VM}{\overline{XL}} \tag{31}$$

The pressure drop across the two-phase region is given by

$$DP = (\overline{\rho_g} \times \overline{XG} + \rho_L \times \overline{XL} + GTPFA) \times LK \tag{32}$$

And the pressure at the top of the mixture by

$$PT = PB - DP \tag{33}$$

The surface pressure is calculated by

$$PS = PT - (GMH + GMFA) \times LMA - (GMH + GMFC) \times WD \tag{34}$$

Where GMFA and GMFC are the frictional pressure loss gradients of the mud above the mixture within the annulus and within the choke line, respectively. The length

LMA is defined in figure 12.

The pressure at the subsea wellhead is computed by

$$PW = PS + (GMH + GMFC) \times WD \qquad (35)$$

G) GAS FILLING THE CHOKE LINE

The gas slip velocity inside the choke line is still calculated by equation 17. Here the parameter DO represents the inside diameter of the choke line. Once DI vanishes, the ratio R equals zero and K1 and K2 are .345 and .2 respectively.

The procedure for finding the pressure drop across the two-phase flow region is similar to that explained in the preceding section. The frictional pressure loss calculation inside the two-phase region is split into two parts, annular and choke line.

The average liquid velocity inside the mixture while flowing through the choke line may be estimated by the following equation

$$VLC = \frac{VM \times AC}{CCL \times \overline{XL}} \qquad (36)$$

Where CCL is the choke line capacity.

The average liquid velocity inside the mixture while flowing through the annulus is also calculated by equation 31.

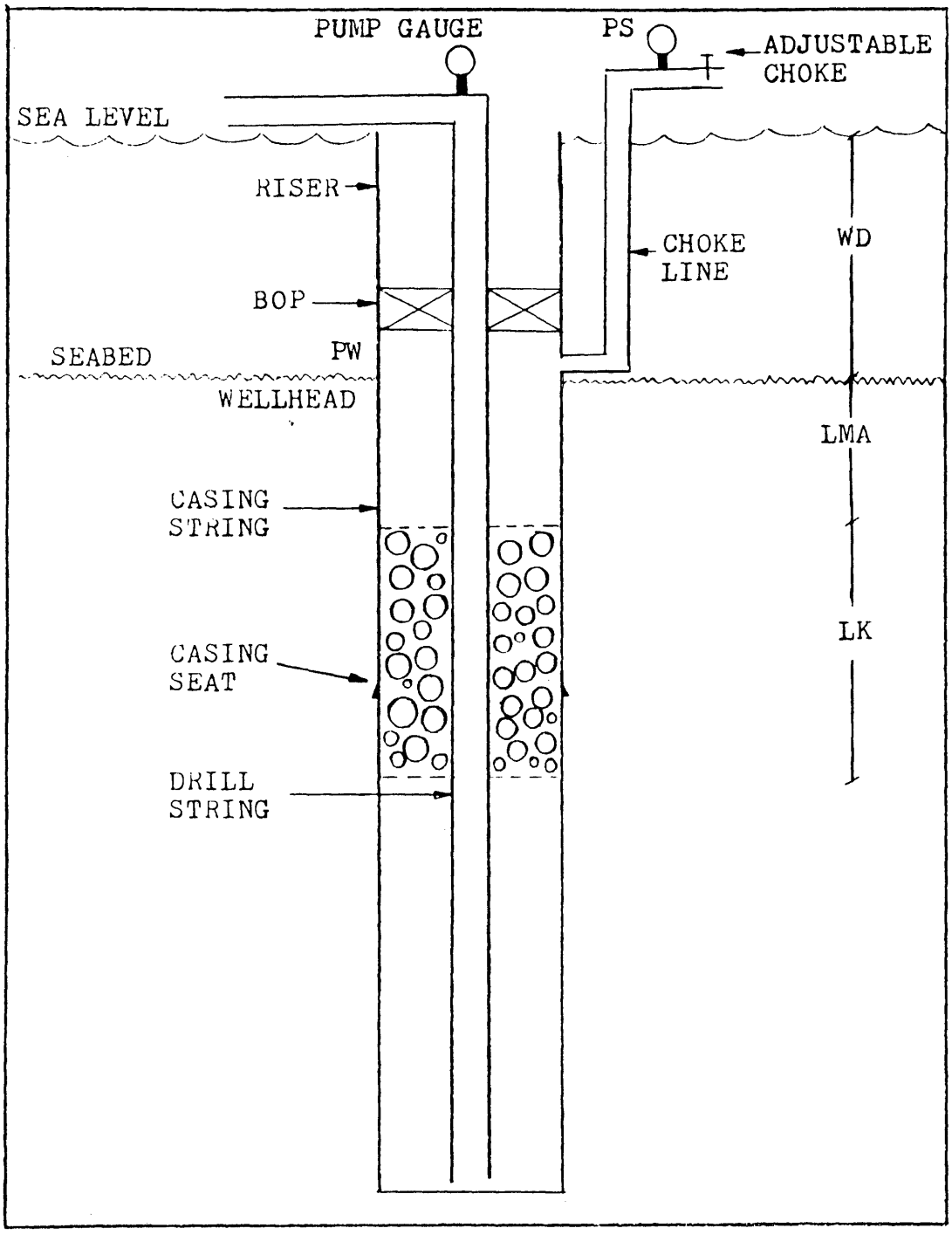

FIGURE 12 - KICK DISPLACEMENT THROUGH THE ANNULUS

The surface pressure is given by

$$PS = PT - (GMH + GMFC) \times (WD - LKC) \qquad (37)$$

The length LKC is defined in figure 13.

The wellhead pressure is defined as

$$PW = PS + (GMH + GMFC) \times (WD - LKC) + (GTPHC + GTPFC) \times LKC \qquad (38)$$

Where GTPHC and GTPFC are the hydrostatic pressure gradient and the frictional pressure loss gradient respectively of the mixture within the choke line.

H) GAS PRODUCTION

During this phase, all gas is removed from the system. Actually this phase comprises two parts. The predominant one represents the gas production from the annulus, ending when the lower boundary of the mixture reaches the choke line. At this time, the second part begins. This part is much shorter than the first one and comprises the production of the remaining gas inside the choke line.

This phase differs slightly from the previous one because the gas mass does not remain constant. The mass rate at which the gas leaves the system is an important parameter that controls the gas properties. A procedure to find this parameter is necessary.

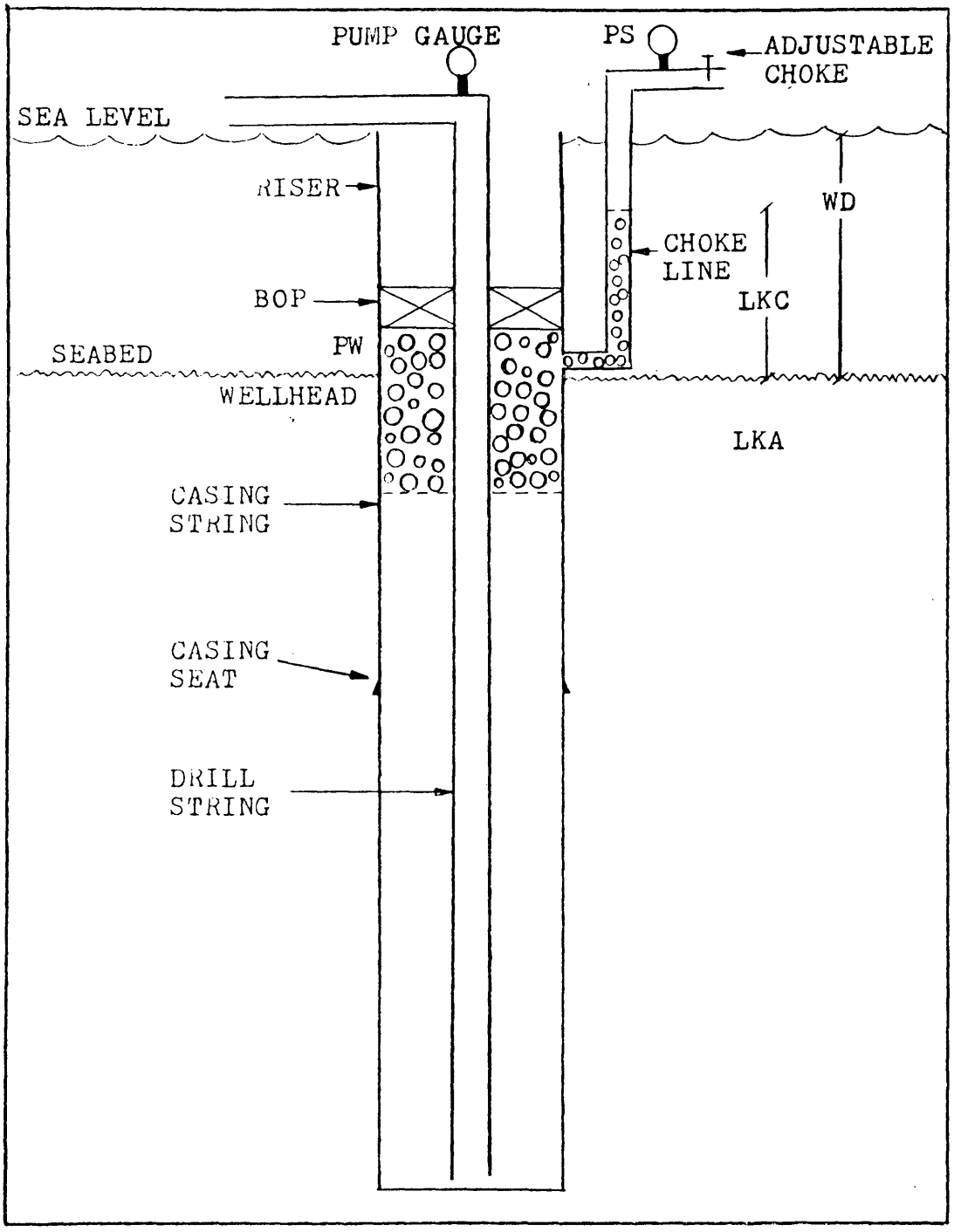

FIGURE 13 - GAS FILLING THE CHOKE LINE

Two reasonable assumptions are considered in order to estimate the rate of mass efflux of gas.

- Bubble diameter is assumed to decrease linearly from a maximum value at the upper boundary to an infinitesimal diameter at the lower end of the mixture. This implies, firstly, the large bubbles are produced, afterward the bubble of medium size and finally the smallest one are produced. As a consequence, the gas mass efflux is greater in the beginning, reducing gradually as the small bubbles arrive at the choke line.
- There is no mass accumulation within the choke line during the gas production, implying that the rate of mass efflux of the gas from the annulus is the same as that from the choke line.

From a continuity equation for a one dimensional flow parallel to the conduit axis (see figure 14), the rate of mass efflux of gas through the section BB' is given by

$$\frac{WI}{TI} = \overline{\rho}_g \times VG \times \overline{XG} \times DA \qquad (39)$$

Where: WI/TI - rate of mass efflux of gas

VG - in situ gas velocity at section BB'.

DA - cross-section area of the duct at section BB'.

The amount of gas that leaves the system is found by multiplying W/TI by the time increment (TI). The gas volume at a certain time within the system is calculated by dividing the remaining gas mass by the average density of the gas. The frictional pressure loss gradient of the mixture used to estimate the mean pressure (equation 25) is given by:

$$\overline{GTPF} = \frac{GTPFA \times LKA + GTPFC \times LKC}{LKA + LKC} \qquad (40)$$

Where: $\overline{GTPF}$ - average frictional gradient

LKA - length defined in figure 15

LKC - length defined in figure 15

Equations 31 and 36 compute the liquid velocities within the annulus and the choke line respectively.

It should be noted LKC is equal to the water depth as long as the gas occupies the annular space.

The surface pressure is now given by

$$PS = PT \qquad (41)$$

The wellhead pressure by

$$PW = PS + (GTPHC + GTPFC) \times WD \text{ , for } LKC \geq WD \qquad (42)$$

And

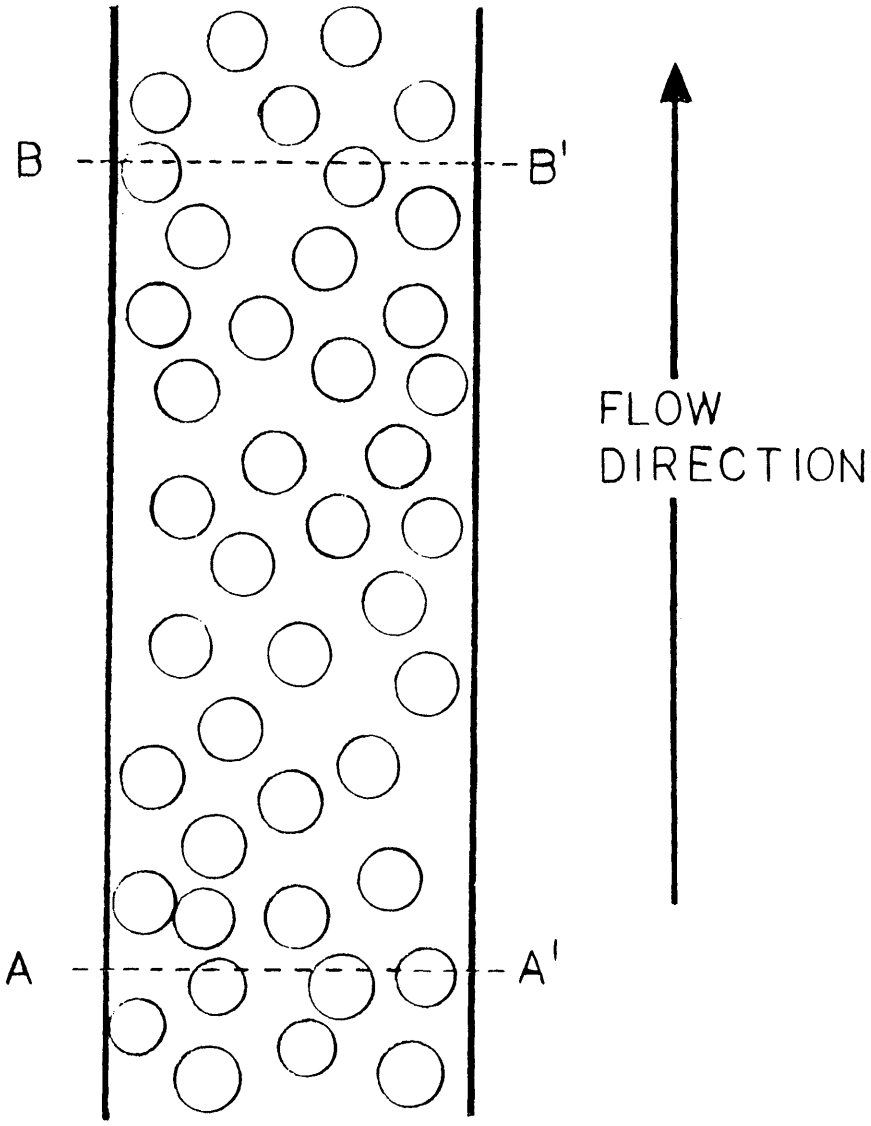

FIGURE 14 - RATE OF MASS EFFLUX OF THE GAS

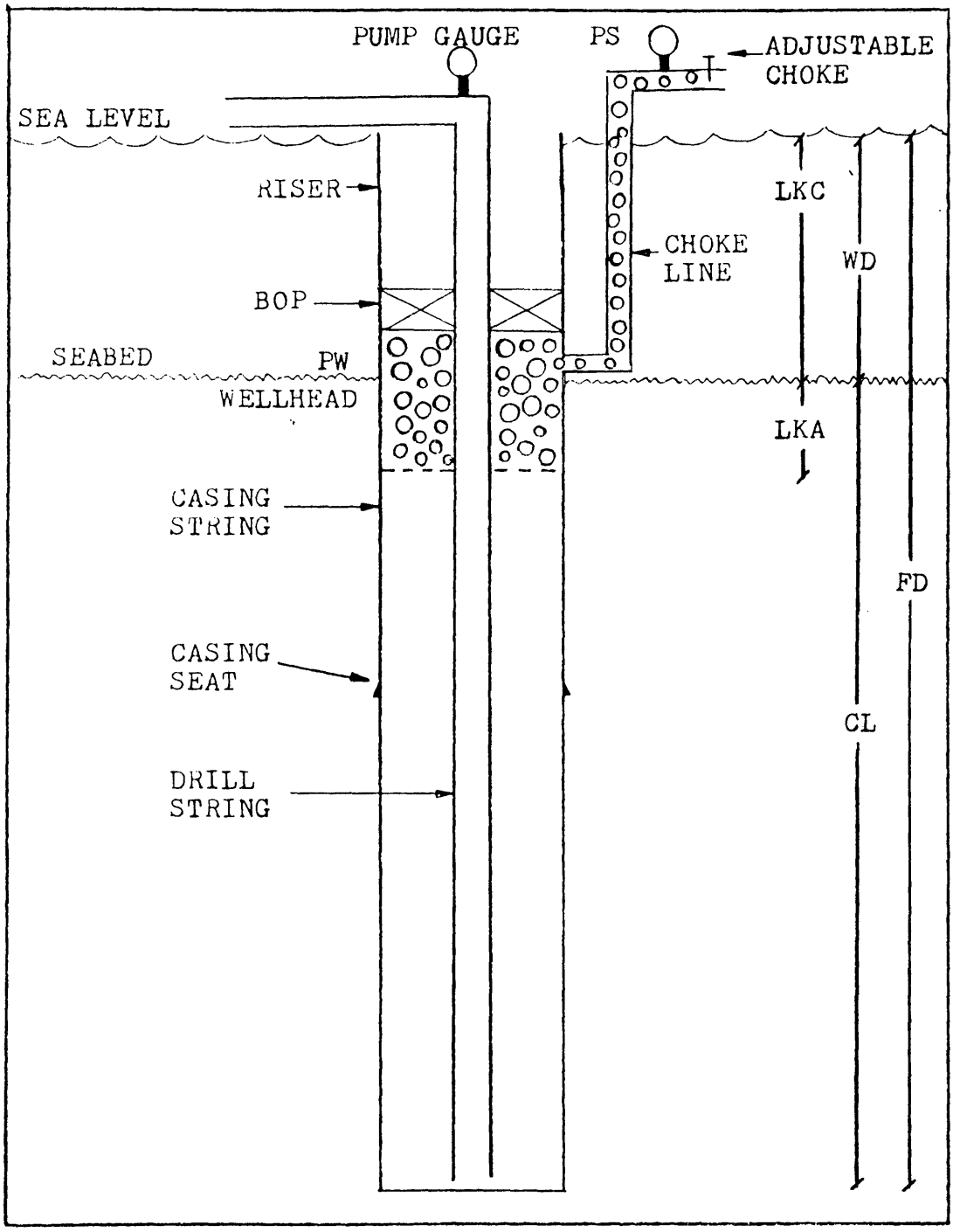

FIGURE 15 - GAS PRODUCTION

$$PW = PS + (GTPHC + GTPFC) \times LKC + (GMH + GMFC) \times (WD - LKC) \text{ , for } LKC \quad WD \tag{43}$$

After all of the gas is out of the system the surface pressure is given by

$$PS = BHP - GMH \times FD - GMFC \times WD - GMF \times CL \tag{44}$$

Where FD and CL are defined in figure 15.

The wellhead pressure is

$$PW = PS + (GMH + GMFC) \times WD \tag{45}$$

I) SURFACE PRESSURE CURVE

A FORTRAN program was written based on the mathematical model described in the preceding sections. The effects of critical variables on the behavior of the surface pressures were studied, one at a time, as the other ones were kept constant.

Figure 16 shows the plotting of surface and wellhead pressure against the time consumed to remove the kick from the well.

The curves in figure 16 were obtained for the following conditions:

Well parameters	
Total depth	10,000 feet
Outer diameter	9.875 inches
Inner diameter	5 inches
Inside choke line diameter	3 inches
Water depth	1000 feet
Water temperature	$50^{o}F$
Geothermal gradient	$.008^{o}F$/foot
Mud parameters	
Density	10 pounds per gallon
Plastic viscosity	15 centipoise
Yield point	10 LBF/100 sq. ft.
Kick parameters	
Kick size	40 barrels
Shut-in drillpipe pressure (SIDPP)	450 psi
Initial average gas fraction	.75
Others parameters	
Gas specific gravity	.65 (air = 1.0)
Reduced circulating rate	200 gpm

These conditions were used as reference for all runs. The above conditions were kept constant, except the one

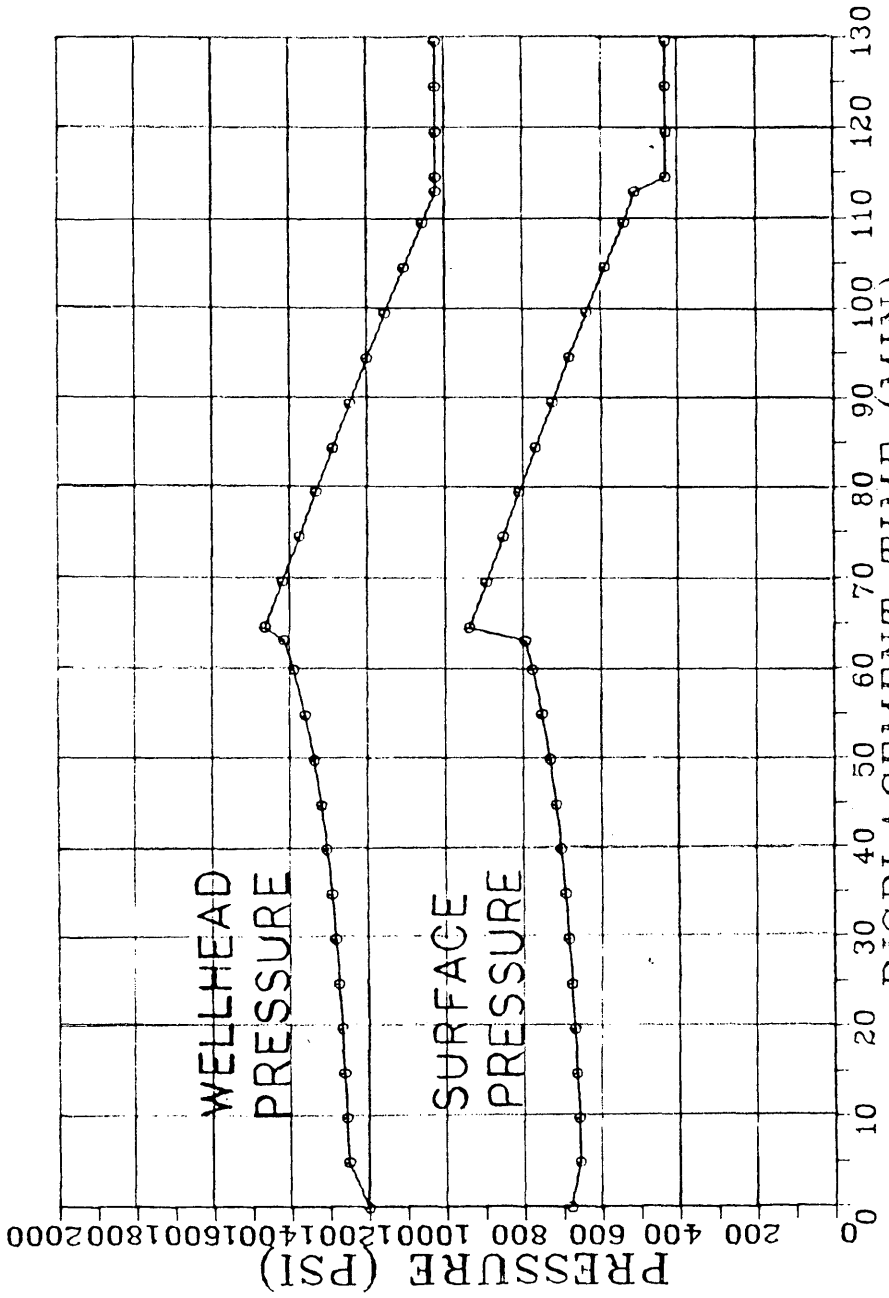

FIGURE 16 - SURFACE AND WELLHEAD PRESSURE CURVES

that was selected for analysis.

The results attained using this model showed a lower maximum surface pressure than that predicted by other models discussed in the literature. The gas is dispersed through the mud, and the hydrostatic pressure variation when the gas enters choke line is not so drastic. Also, the frictional pressure loss inside the two-phase flow region contributes to reduce the maximum surface pressure.

RESULTS

Several situations were simulated for which one variable was varied. These variables were classified into three groups considering the importance of their effect on pressure behavior during kick removal.

A) INITIAL AVERAGE GAS FRACTION

Initial average gas fraction and the minimum diameter of the bubble are intrinsically related to the bubble flow, therefore they were studied more extensively than the others.

Figures 17, 18 and 19 show the effect of the initial average gas fraction on the surface pressure curves. This variable can be thought of as the measurement of the celerity in which the gas flows into the wellbore when compared with the normal circulating flow rate.

From the figures referred to above, it can be concluded that the initial average gas fraction slightly affects the behavior of the surface pressure at deeper well depth. This effect becomes more notable as the well depth reduces.

Because the difference of velocities of the two boundaries is significant, the average gas fraction falls rapidly to a low value, almost independently of the initial average gas fraction. For a shallow well the time

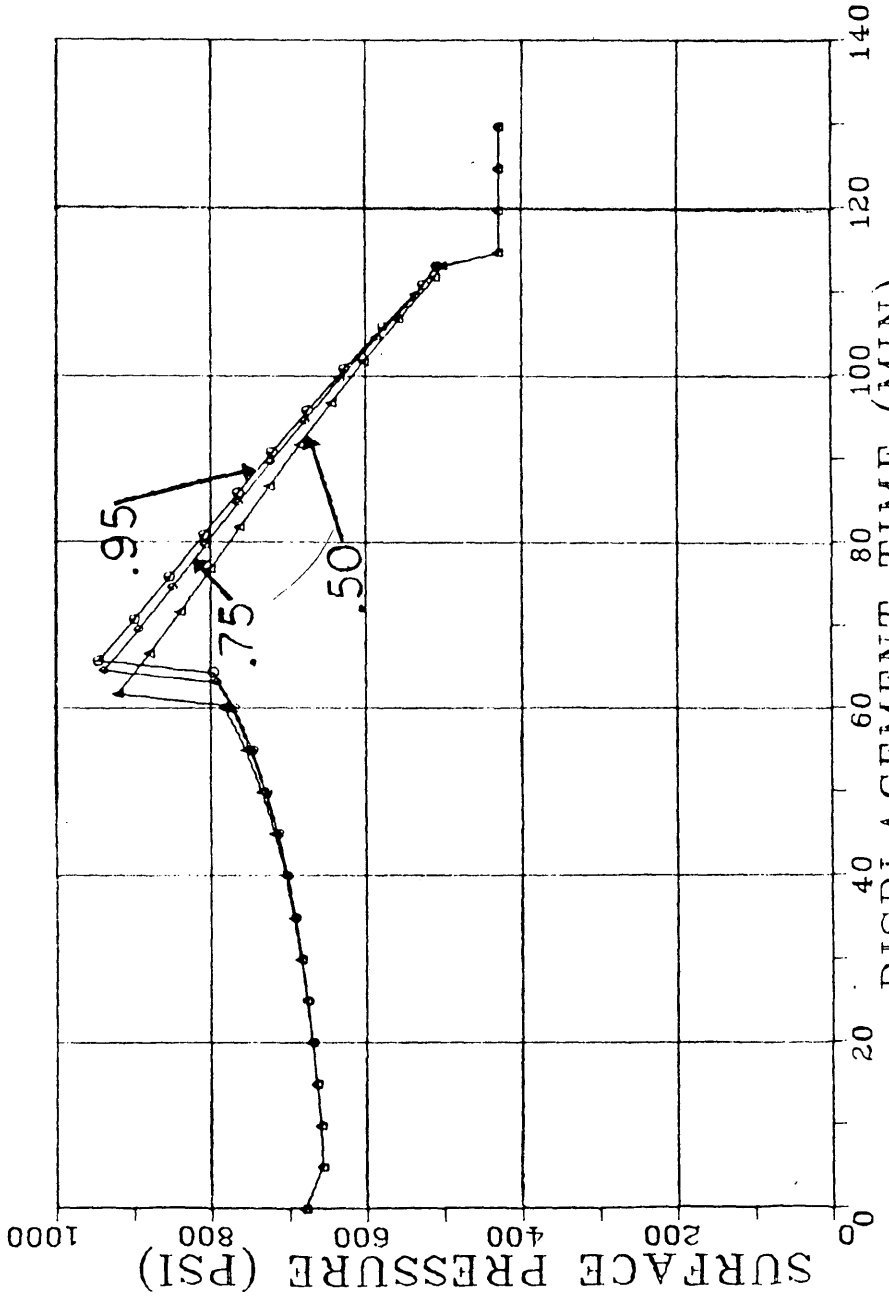

FIGURE 17 - INITIAL AVERAGE GAS FRACTION EFFECT
WELL DEPTH - 10000'

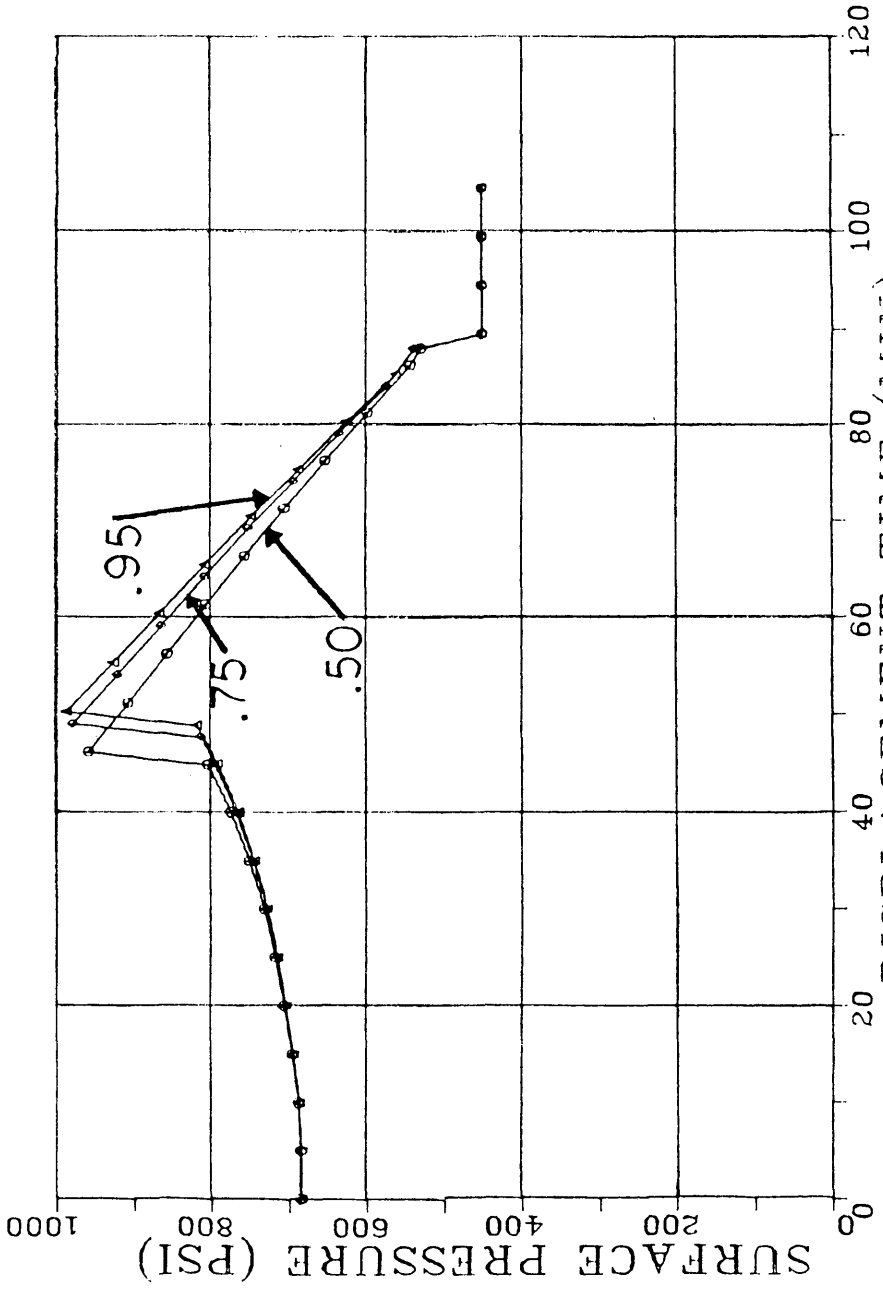

FIGURE 18 - INITIAL AVERAGE GAS FRACTION EFFECT
WELL DEPTH - 8000'

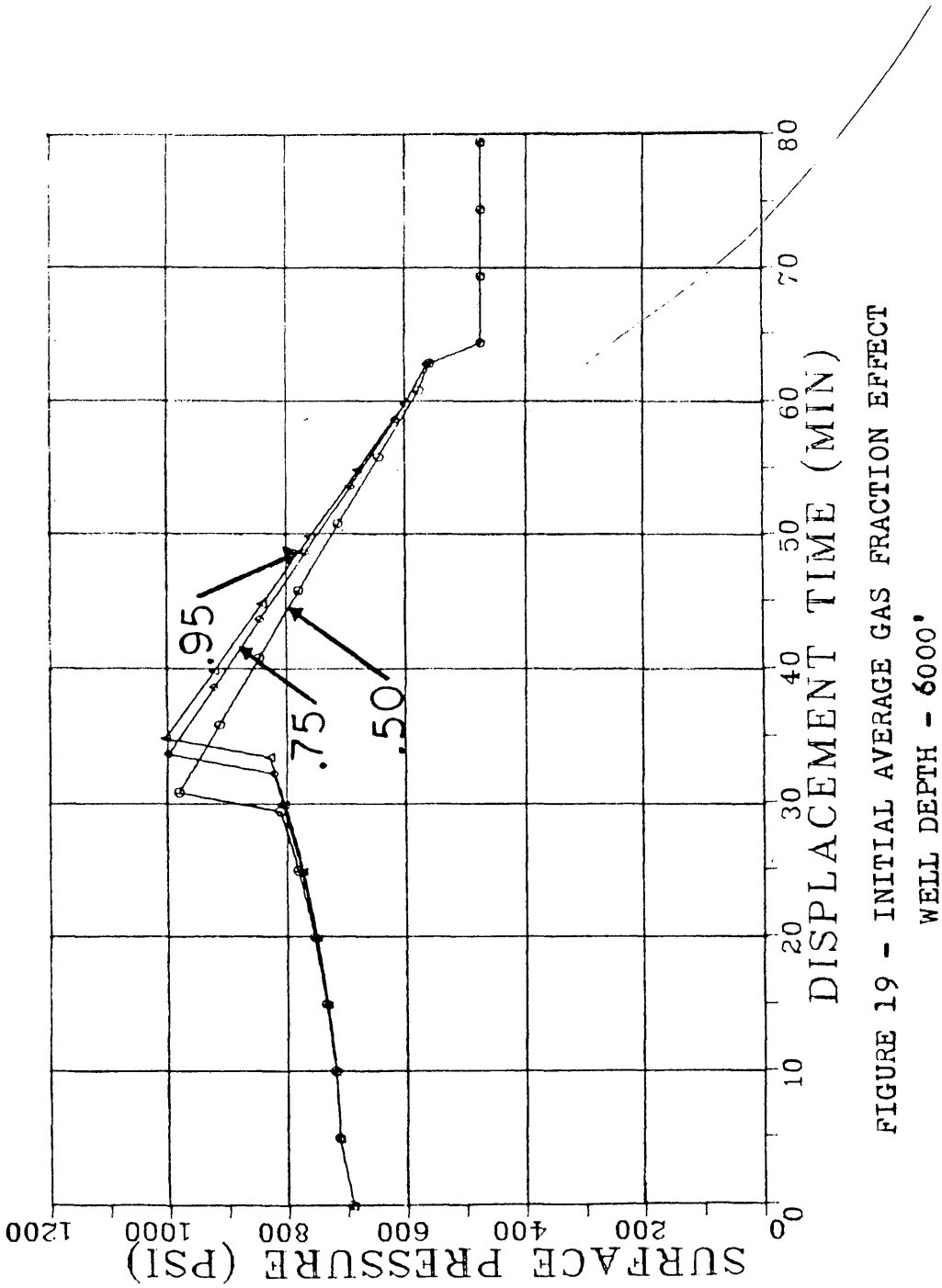

FIGURE 19 - INITIAL AVERAGE GAS FRACTION EFFECT
WELL DEPTH - 6000'

allowed for gas dispersion through the mud is less than that for a deeper one. As a consequence, the initial average gas fraction effect becomes more notable.

At the same well depth, for the lowest initial average gas fraction, the gas kick reached the base of the choke line within the shortest period of time and produced the lowest maximum surface pressure. According to equation 3, the initial length of the kick is related inversely to the initial average gas fraction. This means for a lower average gas fraction, the length of the kick will be larger. As a consequence, for the lowest initial average gas fraction tested in this work, the resultant kick length was the greatest one. Also, the period of time consumed for the kick to reach the base of the choke line was the shortest. The gas bubbles inside the choke line were more dispersed through the mud than in the other tested situations, resulting in the lowest maximum surface pressure.

B) MINIMUM GAS BUBBLE DIAMETER

This variable represents the minimum diameter of the gas bubbles which contributes to the total mass of gas. In other words, the total mass in a bubble which has a diameter less than that minimum is considered negligible. Changes in this variable are useful for testing the

assumption that the lower end of the two-phase region is formed by bubbles of infinitesimal size.

A situation has been simulated in which a bubble diameter of .0039 inches (.1mm) was considered the minimum bubble diameter dispersed through the mud. The results from figure 20 show almost no difference when the minimum bubble diameter is sharply increased from the infinitesimal size to .0039 inches. Consequently, the assumption which considers the lower boundary formed by bubbles of infinitesimal size is valid.

C) KICK SIZE

Kick size, along with the amount of differential pressure during the gas influx, is the most important variable in kick removal.

Figure 21 illustrates the surface pressure curves when kicks of 10, 40 and 70 barrels are taken.

D) MUD DENSITY

The mud density at the time of the gas influx is a very important variable because it acts in two different ways.

Firstly, it determines the amount of differential pressure involved. The gas influx is proportional to this differential pressure raised to the second power. Therefore at a low mud density the volume of gas entering the

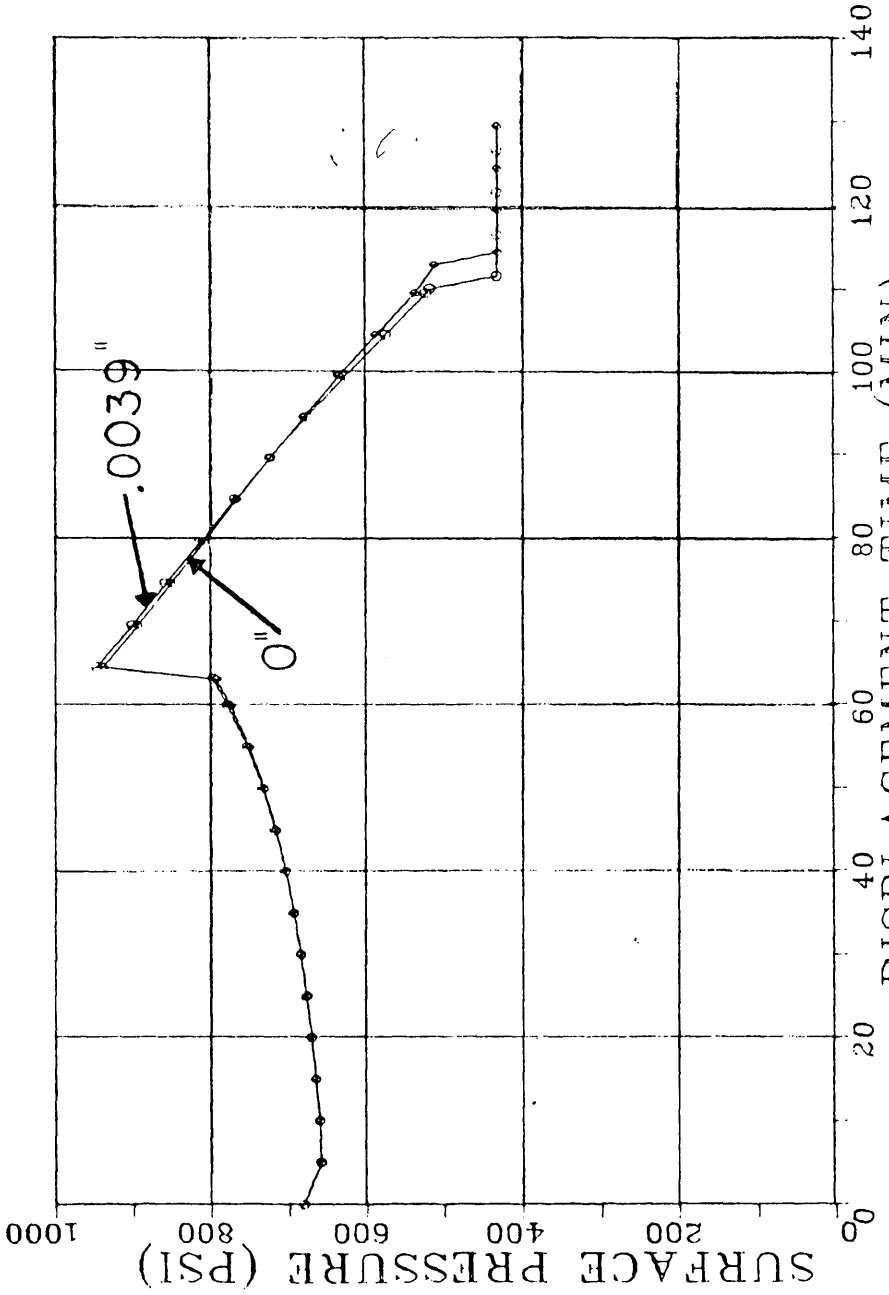

FIGURE 20 - MINIMUM GAS BUBBLE DIAMETER EFFECT

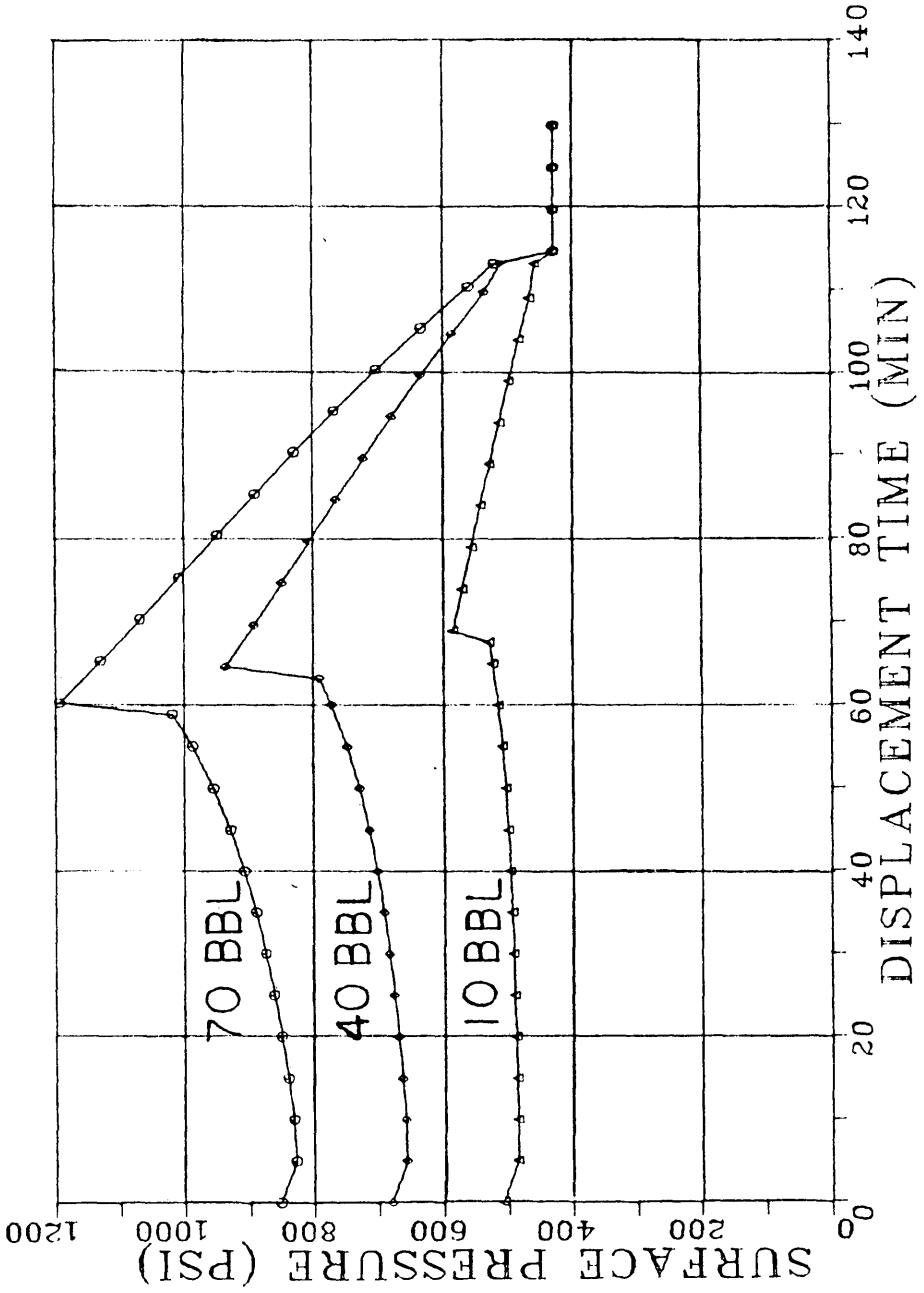

FIGURE 21 - KICK SIZE EFFECT

wellbore is expected to be high.

Secondly, the hydrostatic pressure and frictional pressure loss (when in turbulent flow) are directly proportional to the mud density.

Figure 22 shows three situations:

Mud density	SIDPP
10 ppg	450 psi
10.5 ppg	190 psi
9 ppg	970 psi

It should be noted that a variation of 1 ppg in the mud density caused a remarkable change in the surface pressure behavior.

E) ANNULUS GEOMETRY

For continuity considerations, if the outer diameter of the annular space is reduced, the mud velocity will increase. This means that a kick in a smaller annulus area reaches the base of the choke line before one that is flowing through a bigger one. Also, the height of gas inside the system at shut-in condition will be higher in a narrow annulus. This also leads to a higher shut-in pressure. This explains the surface pressure behavior shown in figure 23.

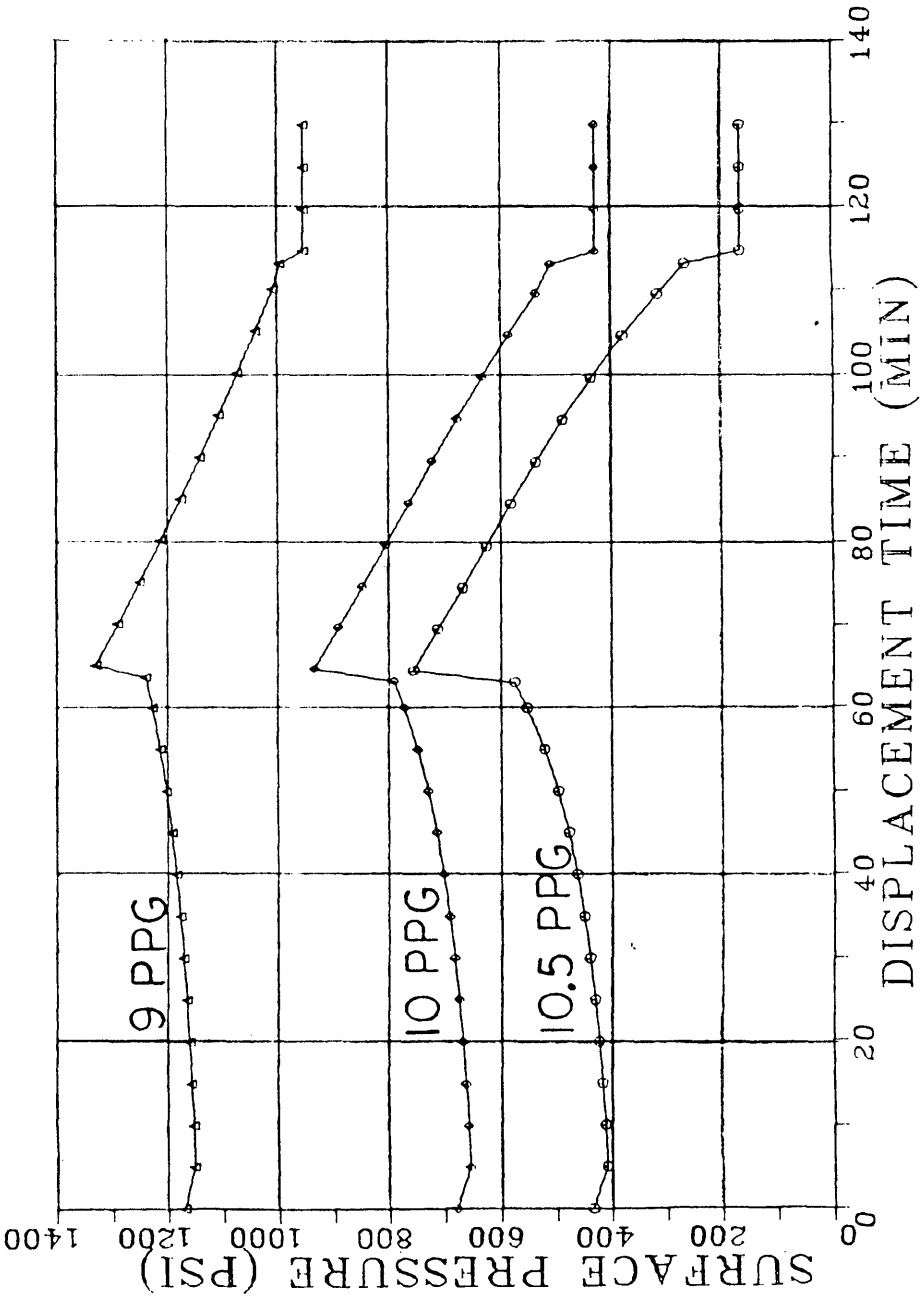

FIGURE 22 - MUD DENSITY EFFECT

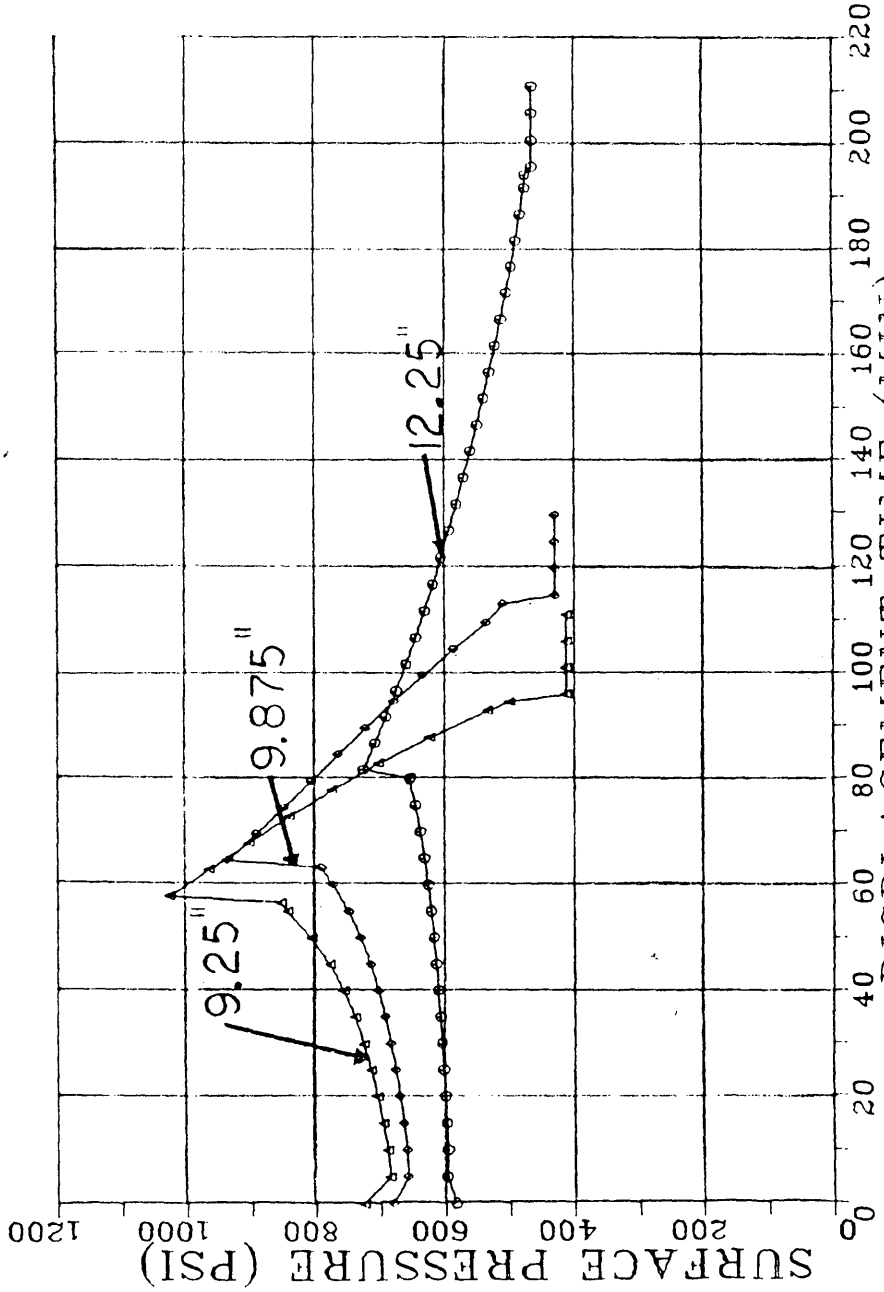

FIGURE 23 - ANNULAR GEOMETRY EFFECT

The gas becomes more dispersed in the mud within a big annular area. This explains why the lowest maximum surface pressure was attained for the biggest annular area.

Another important aspect observed in figure 23 is the rapid change in the surface pressure when the gas enters the choke line and later when it leaves the system. Consequently, the kick displacement becomes difficult to be performed in a small annular area. In this case a lower flow rate could be recommended.

F) WATER DEPTH WITH CONTINUOUS CIRCULATION

The most important effect of increasing water depth was to reduce the surface pressures. The increase in water depth leads to longer choke line and higher frictional pressure loss.

Figure 24 illustrates the surface pressure for three different water depths and one for shallow waters or land drilling; that is, the water depth is zero. The formation depth was considered the same for all water depths studied.

G) CHOKE LINE INSIDE DIAMETER WITH CONTINUOUS CIRCULATION

Smaller inside diameters of choke lines reduce surface pressures. This occurs because of the higher

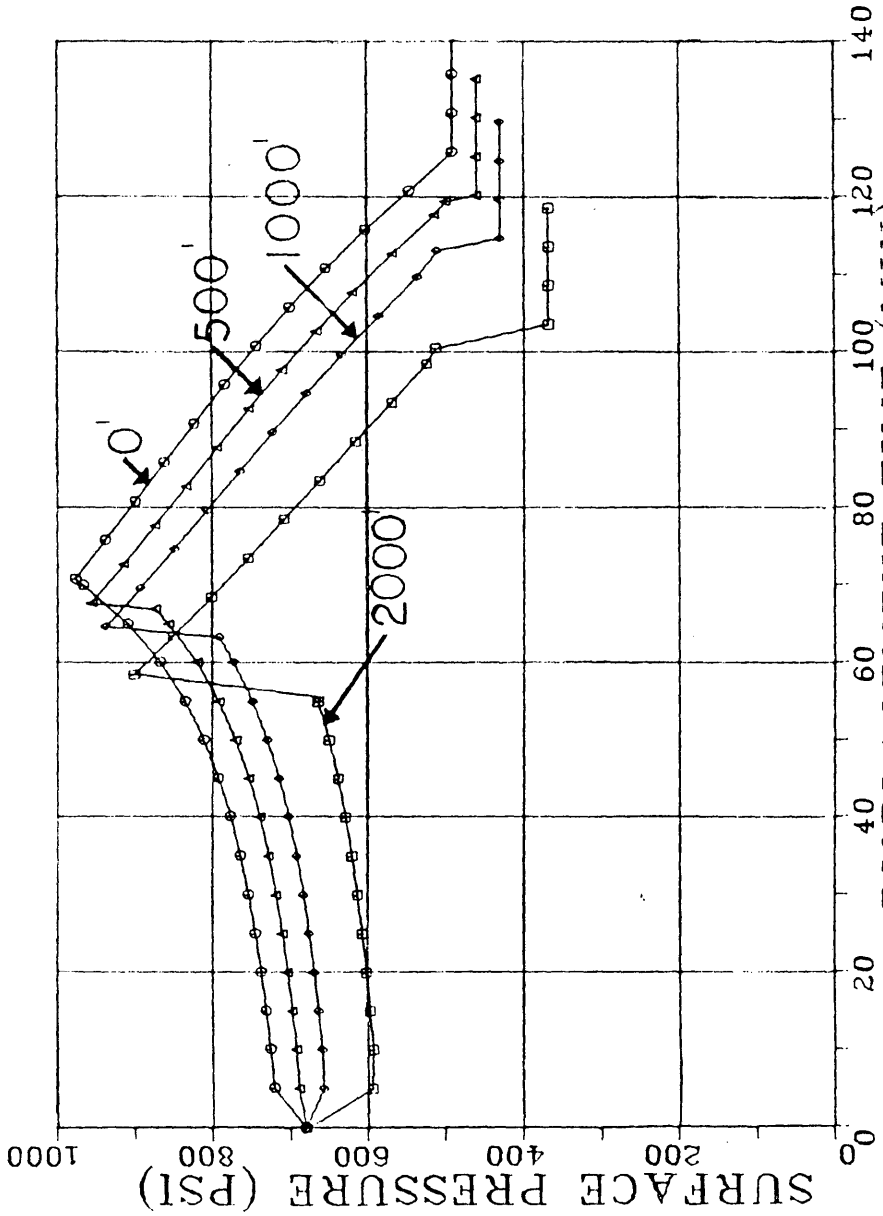

FIGURE 24 - WATER DEPTH EFFECT WITH CONTINUOUS CIRCULATION

frictional pressure losses within the choke line. This behavior is similar to the choke line length effect.

Figure 25 illustrates the surface pressure curve for two choke line inside diameters. The overall effect was to shift down the curves as the inside diameter of the choke line is reduced.

H) RHEOLOGICAL PROPERTIES OF THE MUD

Figure 26 shows the effect of the plastic viscosity and the yield point on the surface pressure profile. The mud properties are listed in table 2.

Mud A is the thinnest one, and therefore yields the least frictional pressure loss. The effect on the surface pressure curve is to displace them down by an amount equal to the difference between the frictional pressure loss generated in each case.

Mud	Plastic viscosity (centipoise)	Yield point (Lbf/100 sq. ft.)
A	5	2
B	15	10
C	40	25

Table 2 - Rheological mud properties

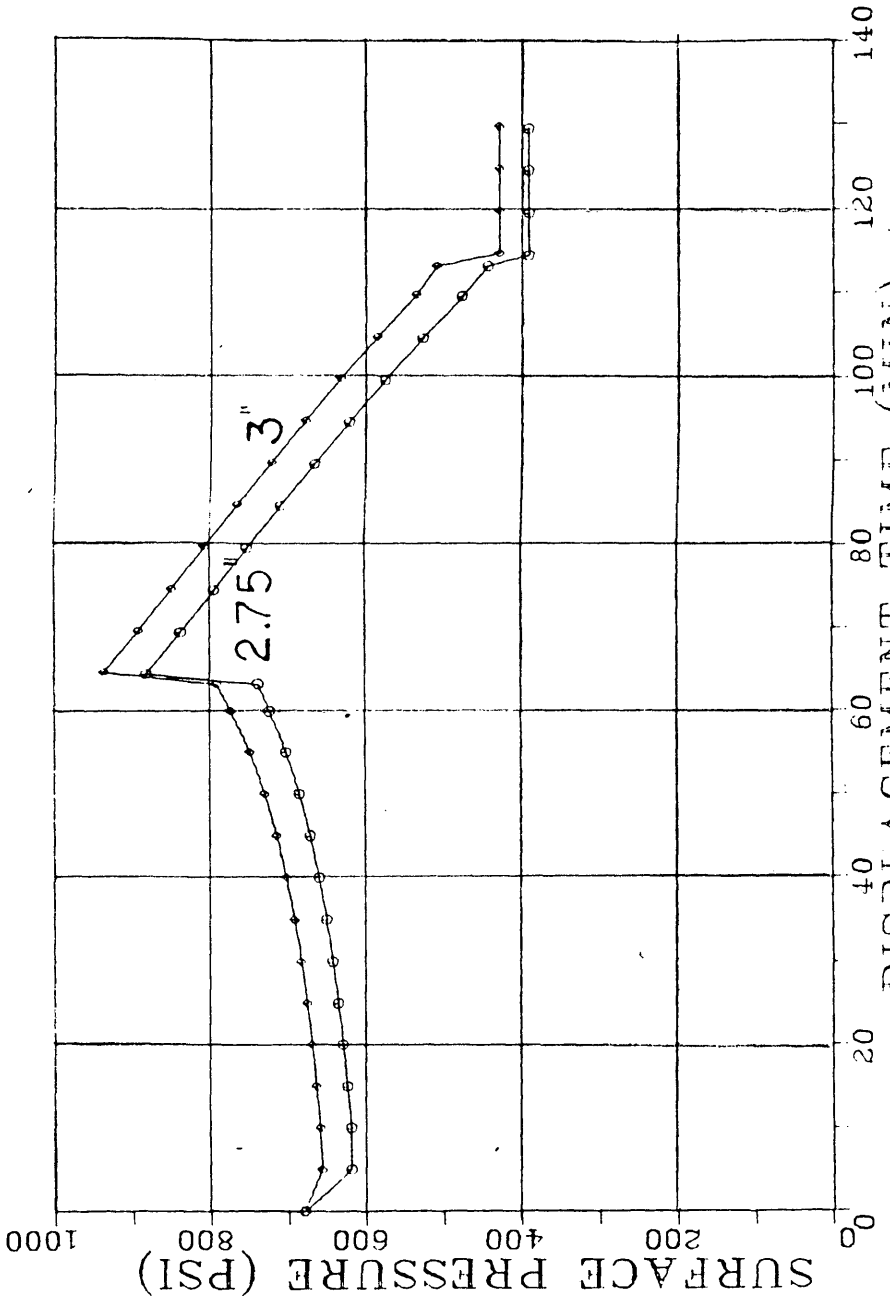

FIGURE 25 - INSIDE CHOKE LINE DIAMETER EFFECT
WITH CONTINUOUS CIRCULATION

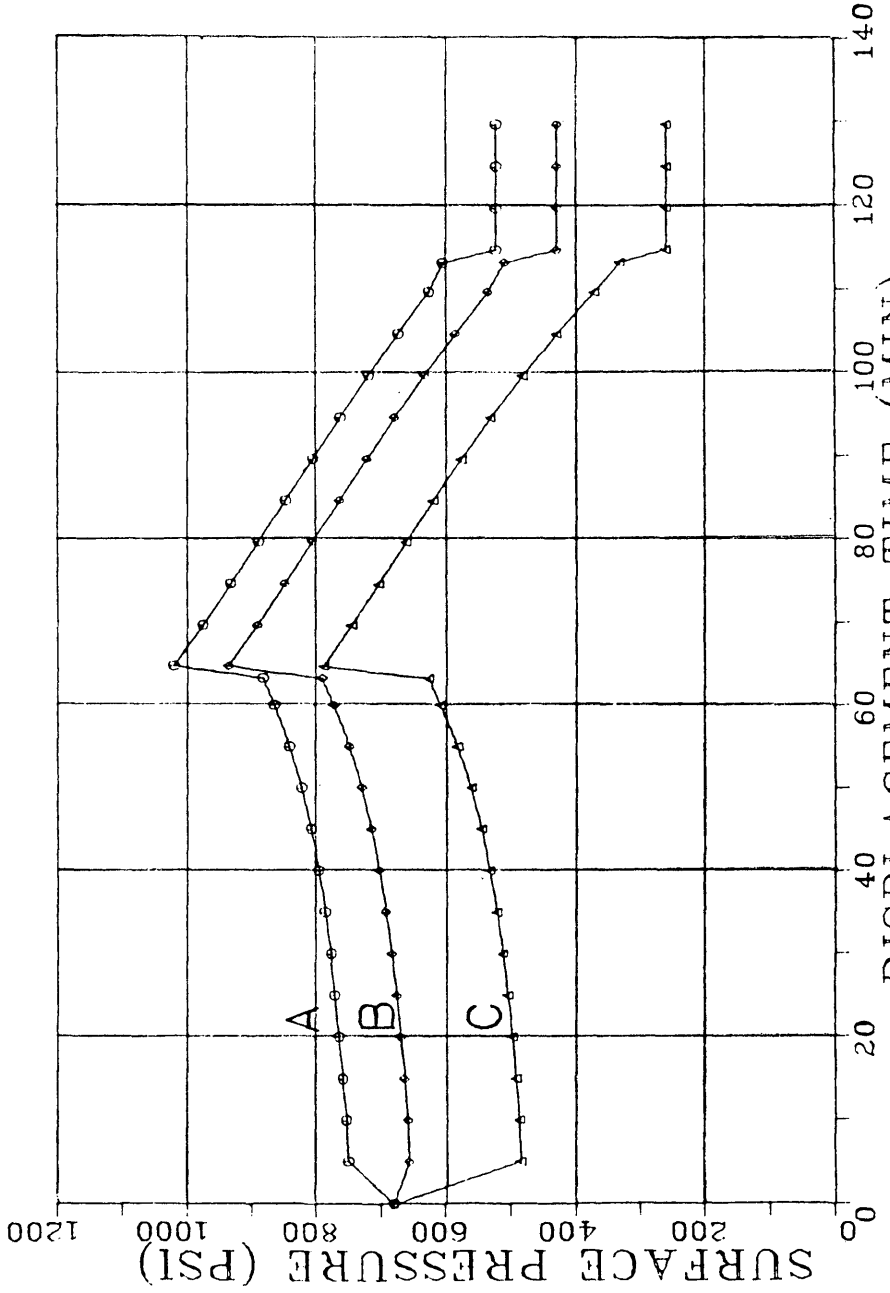

FIGURE 26 - MUD RHEOLOGICAL PROPERTIES EFFECT

I) REDUCED CIRCULATING FLOW RATE

Figure 27 shows the effect of the reduced circulating flow rate on the shape of the surface pressure curves. It is observed that the maximum surface pressures were almost the same for all flow rates tested. The increase in the circulating flow rate results in a higher frictional pressure loss, but at the same time the hydrostatic pressure inside the two-phase region is reduced because the gas has less time to disperse through the mud. The final shape of the surface pressure curve is a balance of these two opposite behaviors.

J) GAS SPECIFIC GRAVITY

Figure 28 shows the slight influence of the gas specific gravity on the surface pressures behavior.

The gas of specific gravity equal to .7 produces a greater hydrostatic pressure than that generated by a .65 specific gravity gas. As a consequence, the .7 specific gravity gas produced a lower surface pressure when compared to the other one.

K) GEOTHERMAL GRADIENT

The temperature gradient through the formations has a negligible effect on the surface pressure curves. Figure 29 illustrates the geothermal gradient effect.

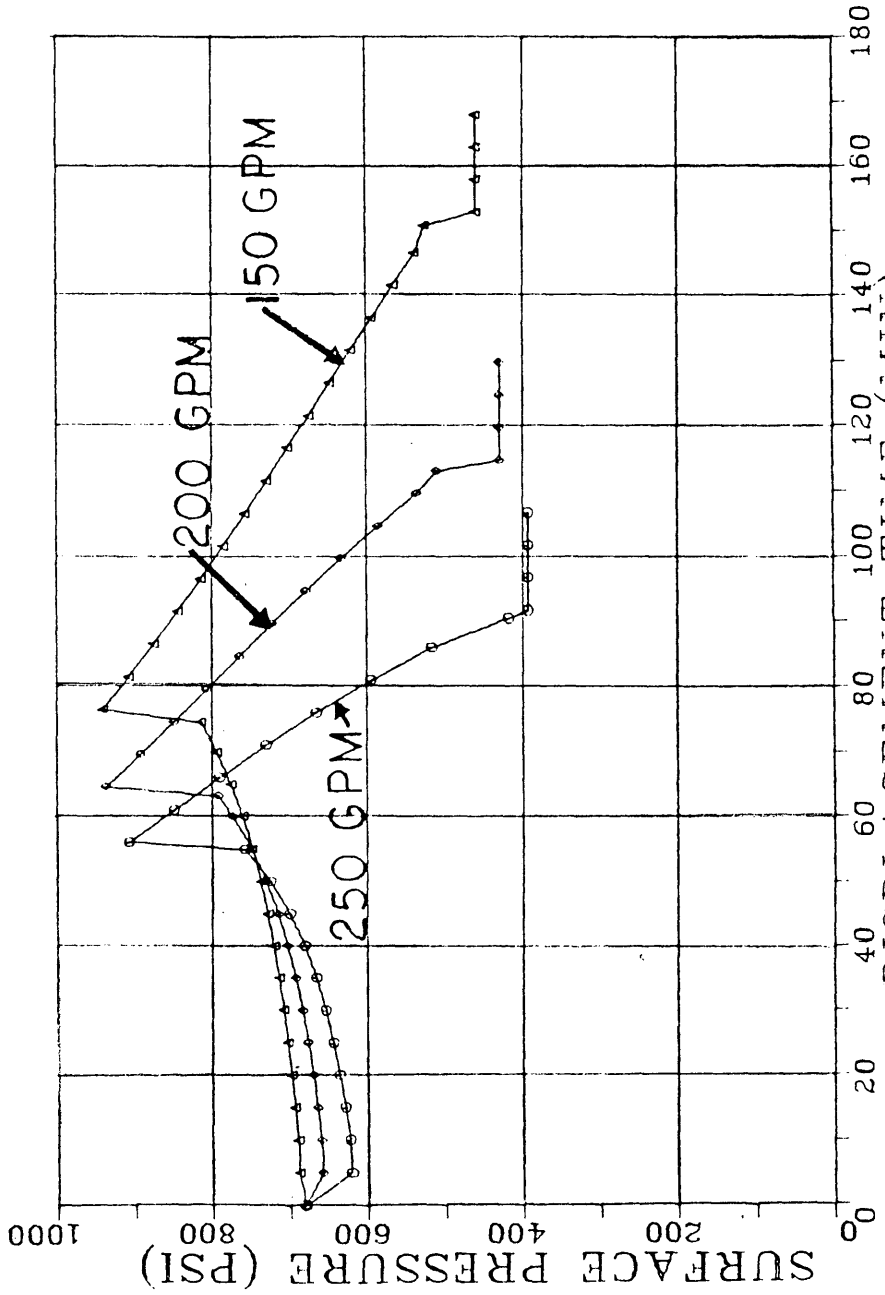

FIGURE 27 - REDUCED CIRCULATING FLOW RATE EFFECT

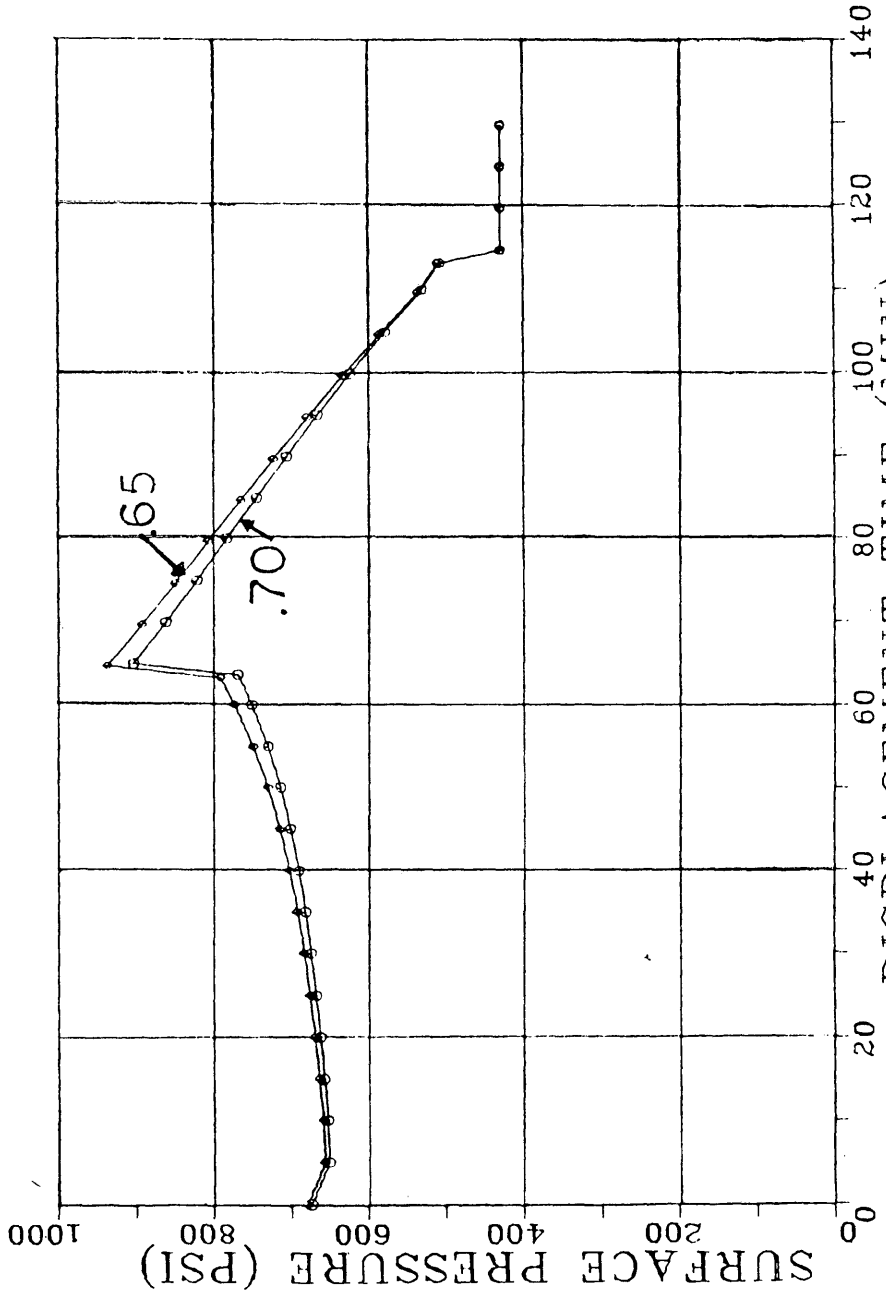

FIGURE 28 - GAS SPECIFIC GRAVITY EFFECT

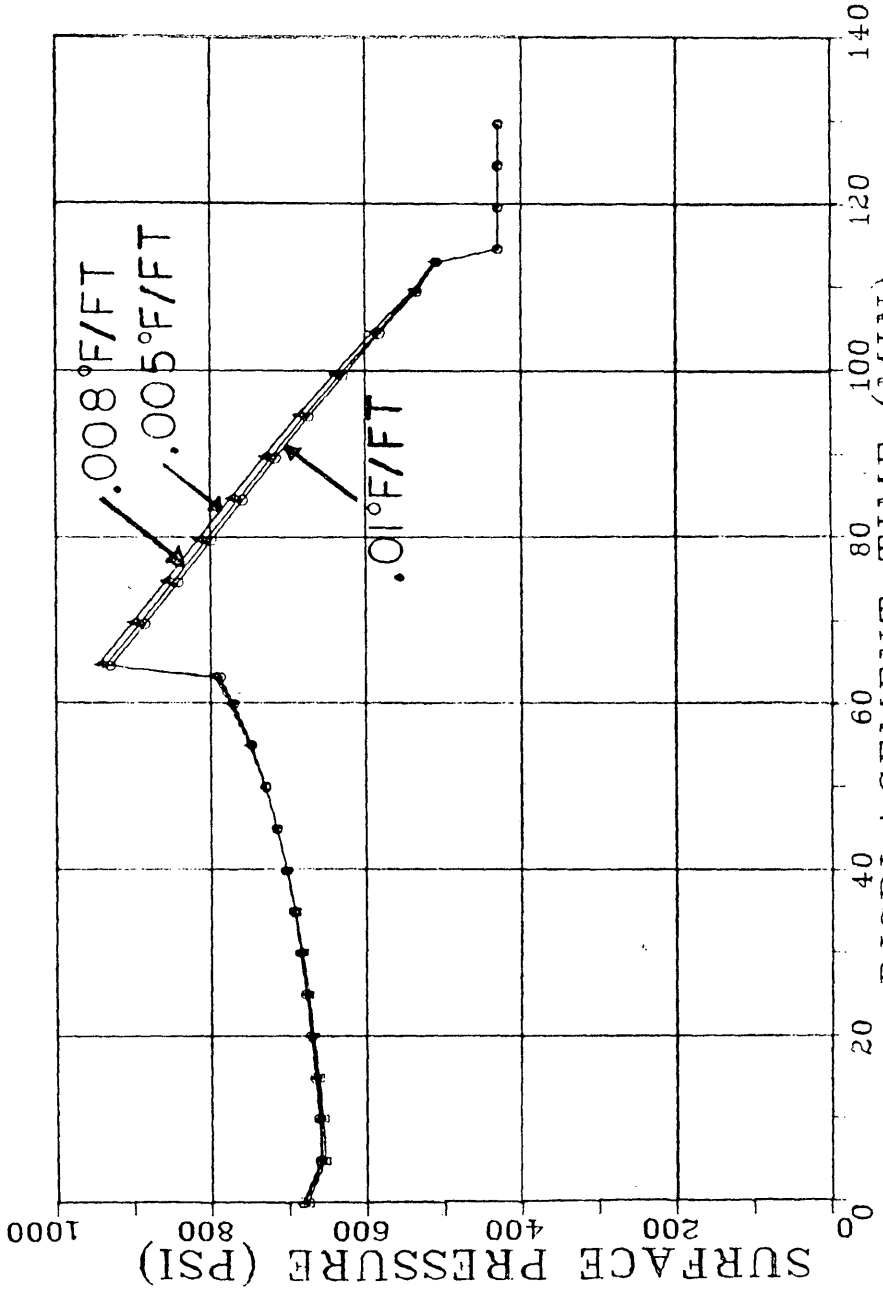

FIGURE 29 - GEOTHERMAL GRADIENT EFFECT

CONCLUSIONS

The conclusions drawn from this work are the following:

1) A mathematical model based on bubble flow pattern can simulate a situation in which the gas has entered the well during normal drilling.
2) Eleven variables have been studied and classified into three groups according to their influences on the surface pressure behavior.
3) Table of Conclusions shows the effect of each variable on the surface pressure behavior.

Variable	Minor effect	Moderate effect	Major effect
Initial average gas fraction	X	X	
Minimum gas bubble diameter	X		
Kick size			X
Mud density			X
Annular geometry		X	
Water depth		X	X
Inside choke line diameter		X	X
Mud rheological properties		X	
Reduced circulating flow rate		X	
Gas specific gravity	X		
Geothermal gradient	X		

Table 3 - Table of Conclusions

REFERENCES

1. Chilingarian G. V. and Vorabutr, Drilling and Drilling Fluids, Amsterdam, The Netherlands, Elsevier Scientific Publishing, (1981)
2. Adams, N., Well Control Problems and Solutions, Tulsa, Oklahoma, Petroleum Publishing Company, (1980)
3. Mitchell, B. J., Well Drilling Handbook, Golden, Colorado, Dr. Bill Mitchell, (1980)
4. Sheffield, R., Floating Drilling: Equipment and Its Use, Houston, Texas, Gulf Publishing Company, (1980)
5. Angel, R. R., Pump Rate and Choke Opening are Varied Together, The Oil and Gas Journal, V. 76, p. 106-109, (1978)
6. Goins, W. C., Kick Control on Floaters Present Unique Problems, World Oil, V. 185, N. 5, p. 47-54, (1977)
7. Craft, B. C., Holden, W. R. and Graves, E. D., Well Design: Drilling and Production, Englewood Cliffs, New Jersey, Prentice-Hall, Inc., (1962)
8. Ilfrey, W. T., Alexander, C. H., Neath, R. A., Tannich, J. D. and Eckel, J. R., Circulating Out Gas Kick in Deepwater Floating Drilling Operations, Paper N^{O}SPE-6834 Presented at the 52nd Annual Fall Technical Conference and Exhibition of the Society of Petroleum Engineers of AIME, Denver, Colorado, (1977)

9. Records, L. R. and Everett, R. H., New Well-Control Unit Speeds Safer Handling of Blowouts, The Oil and Gas Journal, V. 60. p. 106-127, (1962)

10. Lewis, R. L. and LeBlanc, J. L., A Mathematical Model of a Gas Kick, V. 20, P. 888-898, (1968)

11. Records, L. R., Mud System and Well Control, Petroleum Engineer, V. 44, p. 97-108, (1972)

12. Rader, D. W., Bourgoyne, A. T. and Ward, R. H., Factors Affecting Bubble-Rise Velocity of Gas Kicks, Journal of Petroleum Technology, V. 27, p. 571-584, (1975)

13. Stanbery, S. R., Well Pressure Dynamics Under Impeding Blowout Conditions, PhD Dissertation, U. of Texas, Austin, (1976)

14. Wallis, G. B., One Dimensional Two-Phase Flow, New York, New York, McGraw-Hill Book Company, (1969)

15. Nicklin, D. J., Wilkes, M. A. and Davidson, M. A., Two-Phase Flow in Vertical Tubes, Transaction of the Institute of Chemical Engineers, V. 40, p. 61-68, (1962)

16. Griffith, P. and Wallis G. B., Two-phase Slug Flow, Journal of Heat Transfer, V. 83, p. 307-320, (1961)

17. Rader, D. W., Movement of Gas Slugs Through Newtonian and Non-Newtonian Liquids in Vertical Annuli, M. S.

Thesis, Louisiana State University, Baton Rouge, (1973)

18. Griffith, P., The Prediction of Low-Quality Boiling Void, Journal of Heat Transfer, V. 86, p. 327-333, (1964)
19. Kendal, H. A., Fundamentals of Pressure Control - Part 4, Petroleum Engineer, V. 50, p. 60-82, (1978)
20. Govier, G. W. and Aziz, K., The Flow of Complex Mixtures in Pipes, New York, New York, Van Nostrand Reinhold Company, (1972)
21. Brown, K. E. and Beggs, H. D., The Technology of Artificial Lift Methods, Volume 1, Tulsa, Oklahoma, PennWell Publishing Company, (1977)
22. Orkiszewski, J., Predicting Two-phase Pressure Drops in Vertical Pipes, Journal of Petroleum Technology, V. 19, p. 829-838, (1967)

APPENDIX A

DERIVATION OF THE MEAN PRESSURE AND THE DROP PRESSURE EQUATIONS

This derivation is similar to that used in reference 13, except that a more convenient coordinate system was adopted here.

Assuming that the mixture velocity and consequently the frictional pressure loss gradient are not a strong function of the pressure across the two-phase flow region and establishing that H=0 at the bottom of the well, the pressure gradient inside the two-phase region can be expressed by

$$-\frac{dP}{dH} = \overline{XL} \times \rho_L + \overline{XG} \times \overline{\rho}_g + GTPFA \qquad (A\text{-}1)$$

Where: H - Length of the two-phase region

$\overline{XL}$ - Average liquid fraction

ρ_L - Liquid density

XG - Average gas fraction

$\overline{\rho_g}$ - Gas density

GTPFA - Frictional pressure loss gradient across the two-phase region

The gas density can be expressed as

$$\rho_g = A \times P \qquad (A\text{-}2)$$

Where: A - $(K x \gamma_g) / (T x Z)$

K - Constant independent of the gas

γ_g - Gas specific gravity

T - Temperature

Z - Gas compressibility factor

$$So - \frac{dp}{dH} = \overline{XL} \times \rho_L + \overline{XG} \times A \times P + GTPFA \qquad (A-3)$$

Collecting the terms and integrating the equation (A-3), the following equation is obtained

$$\int_{PB}^{P(H)} \frac{dp}{(\overline{XL} \times \rho_L + \overline{XG} \times A \times P + GTPFA)} = - \int_{O}^{H} dH \qquad (A-4)$$

Where PB is the pressure at the lower end of the two-phase region. The above equation yields.

$$P(H) = \left(PB + \frac{\overline{XL} \times \rho_L + GTPFA}{\overline{XG} \times A} \right) x \left(e^{-(\overline{XG} x \Lambda x H)} \right) - \left(\frac{\overline{XL} \times \rho_L + GTPFA}{\overline{XG} \times A} \right) \qquad (A-5)$$

Defining the mean pressure as

$$\overline{P} = \frac{1}{LK} \times \int_{0}^{LK} P(H) \times dH \qquad (A\text{-}6)$$

Where LK is the length of the two-phase region. Substituting (A-6) in (A-5), the expression (A-7) is found

$$P = \frac{1}{LK} \times \left[\int_{0}^{LK} \left(\frac{\overline{XG} \times A \times PB + XL \times \rho_L + GTPFA}{\overline{XG} \times A} \times e^{-(\overline{XG} \times A \times H)} \times dH \right) - \int_{0}^{LK} \frac{XL \times \rho_L + GTPFA}{\overline{XG} \times A} \times dH \right] \qquad (A\text{-}7)$$

Solving the above expression the final mean pressure equation is determined.

$$P = -\frac{1}{LK \times \overline{XG} \times A} \times \left(PB + \frac{\overline{XL} \times \rho_L + GTPFA}{\overline{XG} \times A} \right) \times \left(e^{-(\overline{XG} \times A \times LK)} - 1 \right) - \left(\frac{\overline{XL} \times \rho_L + GTPFA}{\overline{XG} \times A} \right) \qquad (A\text{-}8)$$

The pressure drop equation is derived considering equation (A-5). The pressure at the bottom end of the two-phase region is given by

$$PB = \left(PB + \frac{\overline{XL} \times \rho_L + GTPFA}{\overline{XG} \times A} \right) - \frac{\overline{XL} \times \rho_L + GTPFA}{\overline{XG} \times A} \qquad (A\text{-}9)$$

And the pressure at the top end can be found by

$$PT = \left(PB + \frac{\overline{XL} \times \rho_L + GTPFA}{\overline{XG} \times A} \right) \times \left(e^{-(\overline{XG} x A x LK)} \right) - \left(\frac{\overline{XL} \times \rho_L + GTPFA}{\overline{XG} \times A} \right) \qquad (A\text{-}10)$$

Subtracting (A-10) from (A-9) and defining DP as PB-PT an expression for the pressure drop across the two-phase region is attained.

$$DP = \left(PB + \frac{\overline{XL} \times \rho_L + GTPFA}{\overline{XG} \times A} \right) \times \left(1 - e^{-(\overline{XG} x A x LK)} \right) \qquad (A\text{-}11)$$

This expression can be improved considering that

$$P = \frac{DP}{\overline{XG} \times A \times LK} - \frac{\overline{XL} \times \rho_L + GTPFA}{\overline{XG} \times A} \qquad (A\text{-}12)$$

So the final form of the equation for the drop pressure across the two-phase region is

$$DP = (\overline{P} \times \overline{XG} \times A + \overline{XL} \times \rho_L + GTPFA) \times LK \qquad (A\text{-}13)$$